LUT UNIVERSITY
LUT School of Energy Systems
LUT Mechanical Engineering

Ari Partti

DESIGN OF BOGIE JOINT

7.1.2019
Examiners: Professor Timo Björk
D. Sc. (Tech.) Hannu Oja

TIIVISTELMÄ

LUT-yliopisto
LUT Energiajärjestelmät
LUT Kone

Ari Partti

Telinivelen suunnittelu

Diplomityö

2019

76 sivua, 46 kuvaa, 12 taulukkoa ja 4 liitettä

Tarkastajat: Professori Timo Björk
TkT Hannu Oja

Hakusanat: FEA, kiskorata, teli, telinivel, vinoon ajo

Tämän diplomityön tavoitteena oli löytää uusi ratkaisu tietyntyyppisen nostolaitteen telinivelelle. Uuden telinivelen tuli sallia pyöriminen niveleen asetetun pystysuuntaisen akselin ympäri, sallien suurempia vaihteluita nostolaitteen kiskoradan suoruudessa.

Telinivelelle kohdistuva kuormitus saatiin selville FEA-laskennan tuloksista. Laskennassa käytettiin nostolaitteen palkkielementtimallia ja mielenkiinnon kohteena oli vaakasuuntainen kiskoradan kiskon kyljen ja pyörän laipan välinen tukireaktiovoima, koska tämän vaakasuuntaisen voiman todettiin tekevän nostolaitteesta epästabiilin. Suurin vaakasuuntainen kuormitus johtui pakotetusta nostolaitteen vinoon ajosta ja tätä kuormitusta käytettiin mitoituskriteerinä staattisessa kuormituksessa. Väsymislaskentaa varten luotiin yksinkertaistettu kiskon mutkaisuutta kuvaava malli, jossa kiskon sivupoikkeamien suuruus ja määrä perustuivat ISO-standardiin. Väsyttävä kuormitus saatiin selville kiskon mutkaisuutta kuvaavan mallin aiheuttamien pakkosiirtymien tukireaktioista hyödyntäen samaa palkkielementtimallia kuin staattisen kuormituksen määrityksessä.

Staattisen ja väsyttävän kuormituksen määrityksen jälkeen alkoi nivelen rakenteita ja komponentteja koskeva systemaattinen tuotekehitysprosessi. Rakenteelle luotiin vaatimuslista, joka koostui kuormankantokapasiteetistä niin staattisessa kuin väsyttävässä kuormituksessa, tilarajoituksista, kokoonpantavuudesta ja huollettavuudesta. Näihin osa-alueisiin liittyvien vaatimusten täyttäviä toimintoperiaatteita luotiin yhteensä kolme kappaletta ja niistä luotiin ratkaisuvaihtoehtoja, joista paras valittiin jatkokehitykseen teknistaloudellisen pisteytyksen avulla.

Valittua ratkaisuvaihtoehtoa jatkokehitettiin ja mitoitettiin aluksi analyyttisin laskuin ja myöhemmin elementtimenetelmän avulla ja työn tuloksena saatiin lopullinen perussuunnitelma uudelle telinivelelle. Ratkaisu soveltuu asennettavaksi uusiin nostolaitteisiin ja myös jo käytössä oleviin. Ratkaisu on myös yleisesti soveltuva muun tyyppisiin rakenteisiin.

ABSTRACT

LUT University
LUT School of Energy Systems
LUT Mechanical Engineering

Ari Partti

Design of bogie joint

Master's thesis

2019

76 pages, 46 figures, 12 tables and 4 appendices

Examiner: Professor Timo Björk
D. Sc. (Tech.) Hannu Oja

Keywords: Bogie, bogie joint, FEA, skewing, travelling track

Objective of this thesis was to find new engineering solution for bogie joint of specified hoisting machine. New joint was required to allow rotation around vertical axis of the joint and thus allowing greater deviations in travelling track.

Loading for the joint was obtained as support reaction force from results of FEA calculation of beam element model of hoisting machine. Horizontal force subjected from sides of rails to the flanges of rail wheels was focused because horizontal loading direction induced risk for instability of the hoisting machine configuration. Worst-case horizontal loading was a result of enforced skewing of the hoisting machine and this loading was later used as a static criterion for dimensioning of structures. For fatigue loading criterion, simplified model of travelling track curvature was created. Frequency and magnitude of curvature were based on ISO standard. Fatigue loading was also obtained as a support reaction force of enforced displacements induced by curves of travelling track.

After loading for static and fatigue cases were obtained, systematic product development process for the joint structures and components was carried out. Requirements for static and fatigue loading capacity, space, assembly and maintenance were considered and working principles created according to requirements. Solution variants based on working principles were created and best solution selected for further development based on technical-economic evaluation.

Selected solution variant was further developed and dimensioned first roughly with analytical calculations and more precise with help of FEA. As a result of this thesis, a definitive layout for a new bogie joint was created. Definitive layout is applicable to be retrofitted to existing machines or to new machines yet to be manufactured. The new joint solution fulfills DOF requirements and can be applied to other types of structures with simple structural changes and low number of additional components.

ACKNOWLEDGEMENTS

I want to thank Konecranes Plc Port Cranes business unit for providing the topic for this master's thesis and personnel of the company involved in the project and the personnel of steel structures laboratory in Lappeenranta. Good spirit, teaching and support of laboratory staff had a great impact on my studies.

Finally, I want to thank my family and friends for support during my studies.

Ari Partti
Hyvinkää 7.1.2019

TABLE OF CONTENTS

LIST OF SYMBOLS AND ABBREVIATIONS

A	Tolerance of span [mm]
A_{fork}	Fork structure cross-section area [mm^2]
A_{rod}	Support rod cross-section area [mm^2]
A_{screw}	Screw cross-section area [mm^2]
A_t	Round tube cross-section area [mm^2]
A_u	U-profile cross-section area [mm^2]
B	Tolerance of horizontal straightness [mm]
b	Tolerance of horizontal straightness related to test length of 2000 mm [mm]
c	Distance from neutral axis [mm]
cd	Crane corner distance [mm]
d	shank diameter of screw [mm]
E	Elastic modulus [GPa]
e	Rail wheel line offset [mm]
$F_{b,Rd}$	Limit design bearing force [kN]
F_{fork}	Fork support force [kN]
F_{rod}	Support rod axial force [kN]
$F_{v,Rd}$	Limit design shear force for the screw [kN]
F_x	Horizontal rail wheel force [kN]
F_y	Vertical rail wheel force [kN]
f_{y_rod}	Support rod material yield strength [MPa]
f_{y_screw}	Screw material yield strength [MPa]
f_{y_t}	Yield strength of round tube material [MPa]
f_{y_u}	Yield strength of U-profile material [MPa]
I_{tube}	Moment of inertia of the cross-section of round tube [mm^4]
I_u	Moment of inertia of the cross-section of U-profile [mm^4]
I_{fork}	Moment of inertia of the fork structure [mm^4]
L	Total travelling distance [km]
L_t	Length of round tube [mm]
L_u	Length of U-profile [mm]
$lim\ \sigma$	Limit design stress [MPa]

M_{max}	Maximum bending moment [kNm]
M_z	Support reaction moment [kNm]
N_{k_t}	Euler's critical buckling capacity for round tube [kN]
N_{k_u}	Euler's critical buckling capacity for U-profile [kN]
N_{Rd_t}	Limiting compressive design force for round tube [kN]
N_{Rd_u}	Limiting compressive design force for U-profile [kN]
N_f	Cycle count for service life of fork structure [pcs]
N_t	Cycle count for service life of round tube [pcs]
N_u	Cycle count for service life of U-profile [pcs]
N_x	Horizontal support force [kN]
N_y	Vertical support force [kN]
r_1	Moment arm [mm]
r_2	Moment arm [mm]
r_3	Moment arm [mm]
S	Span [m]
$Smax$	Maximum allowed span [m]
$Smin$	Minimum allowed span [m]
t	Plate thickness [mm]
W	Bending resistance of fork member [mm^3]
Z	Travelling distance [m]
α_t	Imperfection parameter for round tube
α_u	Imperfection parameter for U-profile
γ_m	Resistance coefficient
γ_{mf}	Fatigue strength specific resistance factor
γ_{sbb}	Specific resistance factor for bolted connections
γ_{sbs}	Specific resistance factor for bolted connections
$\Delta\sigma_c$	Characteristic fatigue strength [MPa]
$\Delta\sigma_{Rd}$	Limit design stress range [MPa]
κ	Reduction factor
λ	Slenderness
ξ	Auxiliary variable
σ_{y_fork}	Yield strength of fork structure material [MPa]
τ	Shear stress [MPa]

CAD	Computer aided design
DOF	Degree of freedom
FEA	Finite element analysis
NLS	Nonlinear spring
PTFE	Polytetrafluoroethylene
RMG	Rail mounted gantry crane
VDI	Verein Deutscher Ingenieure – Association of German engineers

1 INTRODUCTION

This master's thesis was done for Konecranes Plc Port Cranes business unit, headquartered at Hyvinkää Finland. Predecessor of the company, KCI Konecranes, was formed in 1994 when KONE-corporation sold its crane division. Nowadays the whole Konecranes Plc employs approximately 17000 people in 50 countries working in design, manufacturing and service of lifting equipment used in industry, shipyards and ports. Product variety is wide ranging from small workstation lifting systems used for example in automotive industry to the largest scale gantry cranes used in shipyards. Product catalogue covers also rubber tired lift-trucks used in terminals and industry. (Konecranes 2018a.) Research carried out in this master's thesis is related to lowest bogie joint of a RMG (rail mounted gantry crane) which is a crane type used for container handling in ports or inland terminals (Konecranes 2018b). Example of BNSF Railway RMG operating in inland railway container terminal is presented in figure 1.

Figure 1. BNSF Railway RMG operating in railway terminal (The Kansas City Star 2015).

1.1 Motivation and research problem

In theory RMGs travel on straight rails (highlighted with arrows in figure 2) mounted on flat ground. In practice these rails are not completely straight and there is also deviation in the ground level and the distance between the rails can deviate also. These deviations are acceptable within a certain tolerance but if the differences are too great, problems can occur in the structure. It has been noticed that components in the bogie structure (marked with dashed line ellipse in figure 2) will suffer premature damages in terminals where rail tolerances in the plane of ground surface are exceeded. Deviations in the plane of ground surface are problematic because of incapability of existing bogie joints to follow such deviations.

Figure 2. Bogie structure of RMG (Konecranes 2018b).

It has been discovered that due to the rail deviation the most vulnerable part of the bogie assembly is the lower joint between balancing beams and bogies. Principle of the bogie assembly and names of the main components are shown in figure 3. Upper, middle and lower joints are all pin joints allowing rotation around the longitudinal axis of the pins. This means that the small-scale deviations in the ground level are not a problem for the structure but the alternating curvature of the rails and varying distance between the rails causes additional loads for the structure and thereby for the joints.

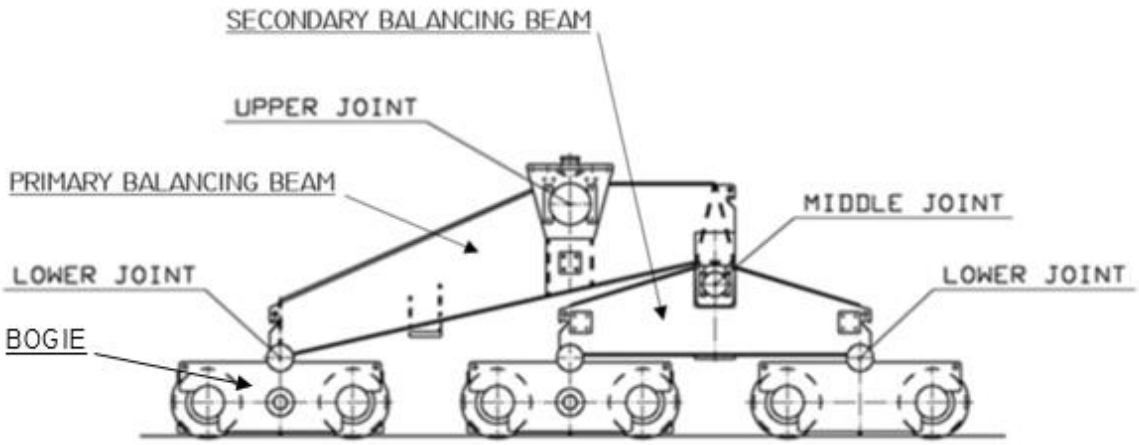

Figure 3. Principle of 6-wheel bogie assembly (Konecranes 2018c).

Geometry of the lower joint differs from the other joints. In the lower joint the pin joint is engineered by using two halves of tube around the pin. Pros of this kind of joint is that components can be assembled just by laying components on top of each other without the need of pushing the pins through aligned holes of lug plates and bogie frame, but the cons are that the combination of additional varying loading caused by rail curvature and geometrical imperfections of the arcs causes the joint to loosen. Arc shaped geometry of the lower joint can be seen in the schematic of bogie frame side view in figure 4.

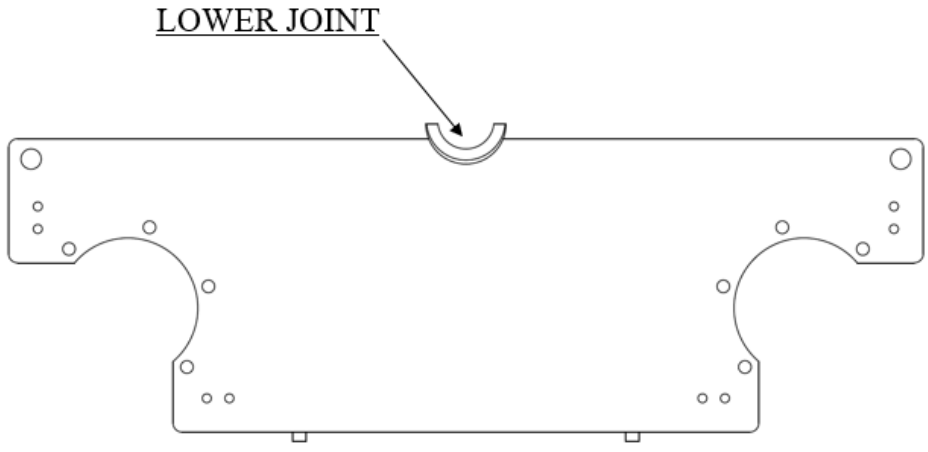

Figure 4. Bogie frame side view and lower joint geometry (Konecranes 2018c).

In addition, for the loosening of the lower joint there are also other problems what the features of the joints enable. As described earlier, the bogie assembly is fundamentally incapable to follow the curves in the rails meaning that the curves of the rails force the bogie assembly to deform to the shape of the rail causing additional stresses to the structure. If the local magnitude of the rail curvature is too great, it is also possible that the bogie assembly will not deform enough causing the outermost wheel to derail.

1.2 Objective and research questions

Objective for this research was to find a new engineering solution for the lower joint and surrounding structure which would allow rotation around the pin axis and in addition for this also rotation around the vertical axis but not around the axis parallel to the movement of the gantry (rail direction). Allowed rotation around the vertical axis would decrease the additional stresses in the joint and in the whole bogie assembly and decrease the risk for derailment due to rail deviations. Research questions used are listed below:

- What is the actual loading with respect to the magnitude of rail deviation?
- What is the best technical-economical solution for the joint?
- How the surrounding structure must be modified to withstand static and fatigue loading of the case?
- What restrictions does the retrofit installation give for the modification of the structure?

1.3 Research methods and structure of the report

Loading cases were determined by using relevant standards and design forces (static and fatigue) for the bogie structure were derived from the loading cases. Conceptual design for the optional solutions was carried out and best option selected with systematic and quantitative method. After the determination of best option for the lower joint, the components and structures included in the whole solution were dimensioned by first narrowing the scale by simple analytical calculations and after that more detailed with computer assisted FEA (finite element analysis). In all calculations requirements for the structures were based on standards. Other reference material used in this thesis in addition to the standards were text books and documentation of the Konecranes company.

1.4 Scope

Research work carried out in this thesis was scoped in a way that possibilities of using so called “pot bearing” (details introduced later) were studied when gathering ideas for the solution which would solve the research problem. Pot bearing supplier was scoped to Freyssinet because of previous research done with the company in question. Other possible solutions engineered with more traditional components were excluded from the research. Basic idea and construction of the bogie structure had to remain the same, only the lower joint and necessary modifications for the steel structure near the joint were the only things allowed to change.

Solution principle for the lower joint had to be scalable to cranes with varying corner loads and wheel quantities. Prototype of the joint solution was designed for one specific RMG crane and testing of the solution will be tested in the future with the crane is question. Relevant details of the RMG crane used in calculations are presented during the report in reasonable sections avoiding detailed description of the engineering solutions. Installation, testing and measurements of the designed joint solution are scoped out from this thesis because of high uncertainty related to timetables of the crane operator. These aspects are considered as a focus point in the future study.

1.5 Contribution

Contribution of this thesis is the methodology of loading definition for the low magnitude rotation allowing lower joint for deflective rails and the definitive layout of the pot bearing lower joint and supporting structure. Same kind of joint could be used in bogies of all types of rail mounted cranes if there is a possibility for deviations in the rail straightness. It must be noted that based on this research the new joint solution cannot be adapted straight to existing or new cranes because the practical tests and verification measurements were scoped out from the research.

1.6 Review of Freyssinet pot bearings

Pot bearing is one type of elastic bearing used in construction industry to carry large vertical loads for example in bridge structures. Other types of these Freyssinet mechanical bearings are elastomeric, spherical and special bearings. Most of these bearing types are used also to carry vertical loads while the configuration of the other constraints varies depending on the

loading case of the structure. Figure 5 presents the constraint configuration principles of mechanical bearings with arrows showing allowed displacements and rotations. From left to right the types of bearings are free, guided and fixed. (Freyssinet 2016.) In this thesis the fixed option of the bearing was the one studied.

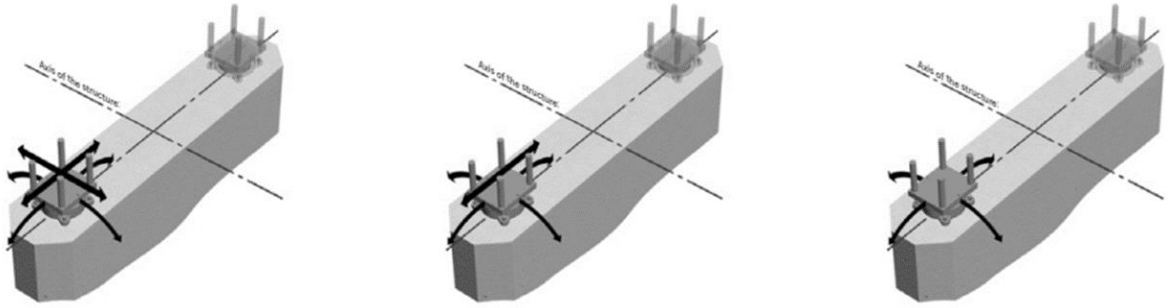

Figure 5. Allowed displacements and rotations of mechanical bearings (Freyssinet 2016).

Example of Freyssinet fixed Tetron CD FX pot bearing is shown in figure 6. Type of the bearing is fixed so vertical and horizontal movement is restricted but rotation around all three axes is allowed. Bearing is built from piston, extrusion seal, elastomeric disc and pot. Elastomeric disc is the key component allowing rotation around horizontal axis. Rotation around vertical axis is enabled by inserting sliding material pair between piston and elastomeric disc. This is not seen in the figure 6. Example of this sliding material pair is thin sheet of stainless steel and PTFE (polytetrafluoroethylene). (Freyssinet 2016.)

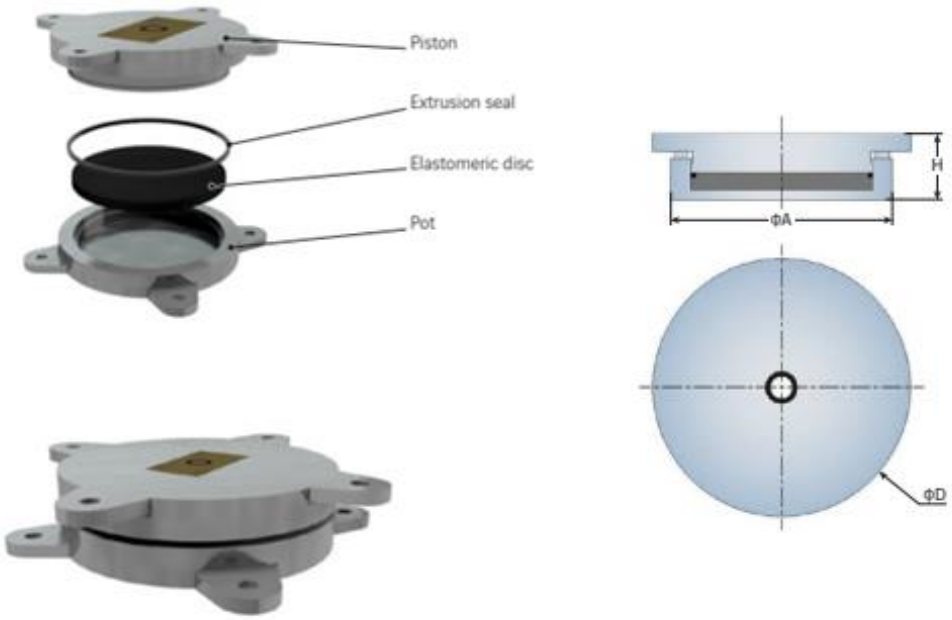

Figure 6. Freyssinet Tetron CD FX pot bearing (Freyssinet 2016).

1.7 Preliminary design

Preliminary design of the lower joint with pot bearing is presented in figure 7. This solution was the base for the whole design work carried out in this thesis and the solution shown in the figure 7 was done before this study started. Coordinate system used in the following sections of this thesis is also seen in the figure.

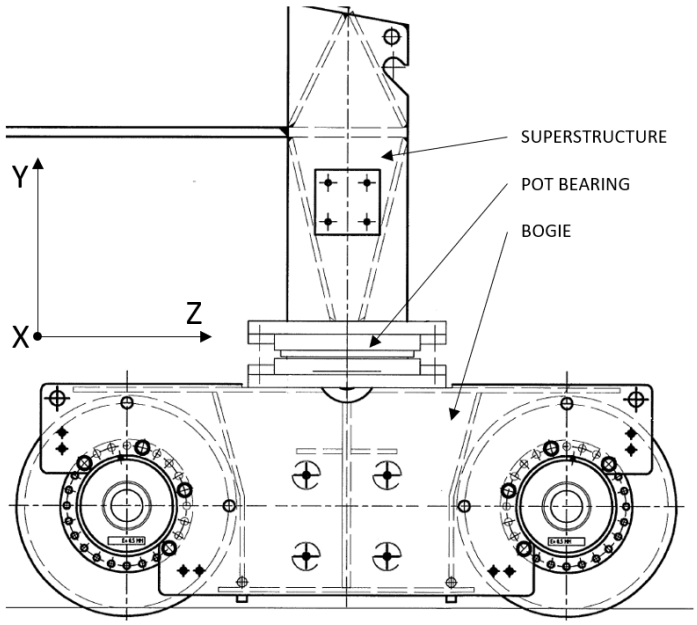

Figure 7. Preliminary design of the pot bearing lower joint (Konecranes 2018c).

2 LOADING OF THE JOINT

To find out the loading in the bogie structures lower joint, basic static equilibrium for the situation was studied. Then the effect of all possible loading cases and their combinations according to standards were considered for the static equilibrium to find out the worst-case loading. FEA was utilized when studying the worst-case load combination for the lower joint. Loading from the results of FEA was then used as a design criterion when static strength of the components and structures was proofed. For fatigue design, load combinations and their frequency of occurrence were studied and simplified model for fatigue design criterion was created. Safety factors were based on limit state method of SFS-EN 13001-1 standard for individual loads and for yield strength of material used. In this chapter forces and their partial safety factors were studied. Safety factor for limit design stress was taken into consideration in the structural design phase. (SFS-EN 13001-1 2015, p. 43-44.)

2.1 Static equilibrium

Static equilibrium of the bogie is presented in figure 8. F_y is the vertical rail wheel force subjected from rail to the rail wheels. This includes the force for both two wheels. F_x is the horizontal rail wheel force subjected from rail side to the rail wheel flanges. These two forces must have support reaction forces in opposite directions. These support forces are vertical support force N_y and horizontal support force N_x. For addition to the forces, the bogie also needs to have support reaction moment M_z around the pot bearing tilting point because otherwise the bogie would collapse under the superstructure. In theory the elastomeric material inside the pot bearing can resist M_z until some point, but in practice the acting forces being so great and resistance of the elastomeric material so low, the bearing was simplified to a spherical joint in sense of degrees of freedom (DOF). N_y, N_x and M_z are only dependent on F_y and F_x meaning that the worst combination and fluctuation of F_y and F_x lead to the design criterion of the joint both in static and fatigue cases. Due to the high vertical load carrying capacity of the pot bearing, study was focused on the horizontal force which is much more crucial for the behaviour of the joint because natural lack of moment resistance of the pot bearing.

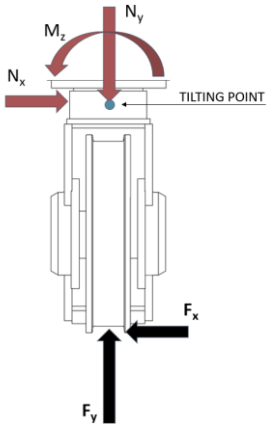

Figure 8. Static equilibrium of the bogie.

2.2 Finite element model

To obtain F_y and F_x, for all twelve lower joints, beam-element model of the gantry was created with FINNGEN 8.0.1 modelling software. FINNGEN is a product of Finnish FEMdata Oy which is used for creating FEA models for actual solver software FINNSAP provided by the same company. Postprocessor software FINNDRAW was used to read the results of the finite element analysis and to present them graphically. (FEMdata 2018.) Basic geometry of the beam element model is shown with rails in figure 9. Constraints and loads are presented in sections 2.7 and 2.8.

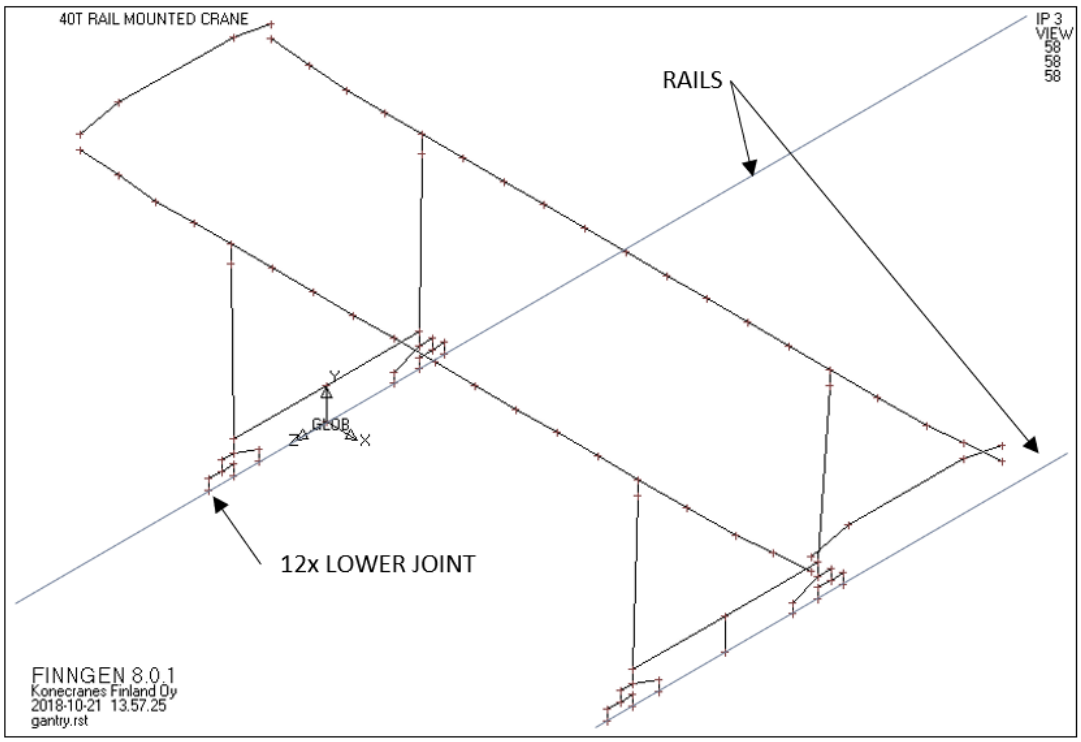

Figure 9. Beam element model of the gantry.

Model was created with the assumption of the use of pot bearing, meaning that in every corner of the gantry there is three loading points presenting the bearings. If rotation around Y-axis wasn't allowed like in the standard design of the bogie, then the lowermost part of the model would be different because of the difference in the DOF.

2.3 Operational loads and load combinations

Operational or regular loads as in standard SFS-EN 13001-2 are the loads acting on the crane structure in normal use of the equipment. In this context normal use means the operational use of the crane without any faults in the components or mechanisms which failure would cause higher stress levels in the crane structure. (SFS-EN 13001-2 2014, p. 94.) Load combinations including only the effects of normal use are called "load combinations A" according to SFS-EN 13001-2 (2014, p. 94). Other widely used standard used in crane design called F.E.M. 1.001 3nd defines the load combinations build from the operational loads as CASE I loading. Description of the CASE I loading is "APPLIANCE WORKING WITHOUT WIND" according to F.E.M. 1.001 3nd. (F.E.M. 1.001 3nd 1998, p. 32.)

Idea behind load combination A and CASE I loading is the same, presenting the loads under normal working cycle. For example, safety and impact factors differ, but the principle for inducing operational loads is the same. Because of the frequency of the operational loads being high compared to other types of loading, fatigue assessment of the crane structure is generally based just on the operational loads (SFS-EN 13001-2 2014, p. 72). Regular loads according to SFS-EN 13001-2 are described in table 1. For making calculation process simpler, effects of uneven travelling surface, displacement induced loads and acceleration related loads were ignored because their low effect to studied load variables. The loads used in the calculations for the lower joint are marked with x.

Table 1. Regular loads and scope for analysis (mod. SFS-EN 13001-2 2014, p. 71).

"a) Hoisting and gravity effects acting on the mass of the crane"	x
"b) inertial and gravity effects acting vertically on the hoist load"	x
"c) loads caused by travelling on uneven surface"	
"d) loads caused by acceleration of all crane drives"	
"e) loads induced by displacements"	

2.4 Occasional loads and load combinations

In addition, for operational loads, there are also occasional loads subjected to the crane structure. Load combinations including the occasional loads are called “load combinations B” according to SFS-EN 13001-2 (2014, p. 94). Load combinations B are the same than load combinations A, with the difference that the effects of occasional loads are added to the load combinations A (SFS-EN 13001-2 2014, p. 94). In F.E.M. 1.001 3nd the occasional loading is defined as CASE II loading. Description of this CASE II loading is “APPLIANCE WORKING WITH WIND” according to F.E.M. 1.001 3nd (1998, p. 32).

In the case of occasional loading, description of the load combination in SFS-EN 13001-2 is wider than in F.E.M. 1.001 3nd because CASE II just adds the in-service wind to the CASE I or load combinations A situation. In practice they still are quite close of each other because of wind with relatively high velocity is considered as in-service wind. This means that in-service wind is quite often the most critical of the occasional loads.

Table 2 presents the occasional loads according to SFS-EN 13001-2. Only loads a) and d) were considered because in general situation snow loads and effects of temperature variations can be ignored because of small areas for snow build up and constraint configuration allowing virtually free expansion due to temperature changes (F.E.M. 1.001 3nd 1998, p. 31). Skewing of the gantry can be occasional or depending on the geometry, mass, rail-wheel contact and other factors also regular load when it should be included in fatigue assessment. In the case of RMG, skewing was considered as occasional because the amplitude of frequent skewing being small due to electronically controlled skewing. (SFS-EN 13001-2 2014, p. 82.)

Table 2. Occasional loads and scope for analysis (mod. SFS-EN 13001-2 2014, p. 71).

"a) Loads due to in-service wind"	x
"b) snow and ice loads"	
"c) loads due to temperature variations"	
"d) loads caused by skewing"	x

2.5 Exceptional loads and load combinations

Third classification for loads is exceptional loads. Exceptional loads are rare, and they are generally left out from the fatigue assessment. Magnitude of exceptional loads is often much

greater than with operational or occasional loads and load combinations. In F.E.M. 1.001 3nd the exceptional loading is defined as CASE III loading. Description of this CASE III loading is "APPLIANCE SUBJECTED TO EXCEPTIONAL LOADINGS" according to F.E.M. 1.001 3nd (1998, p. 33). In SFS-EN 13001-2 (2014, p.94) load combination including exceptional loadings is called "load combination C". According to SFS-EN 13001-2 (2014, p.94) "load combination C cover a selection of regular loads combined with occasional and exceptional loads". Table 3 presents exceptional loads based on the both discussed standards in a summarized form. SFS-EN 13001-2 gives much more detailed explanations for different form of failure than F.E.M. 1.001 3nd but as in the case of operational and occasional loads, the idea and principle behind the classification is the same.

Table 3. Exceptional loads and scope for analysis.

a) Loads due to storm wind	x
b) test loads	
c) loads caused by failure*	x
d) loads caused by buffer effect	

*failure of component or mechanism or failure in lifting or travelling procedure.

2.6 Rail deviations

As an addition for the standardized loads and load combinations, deviations in the travelling tracks are usually left without detailed study. In this study, where rail deviations are the most probable cause for the lower joint wear, the effects of rail deviations were considered when defining fatigue loading for the newly designed structures of lower joint. To be more precise, deviations in the horizontal plane were the focus, because as described earlier, the way of handling of horizontal force F_x dependent M_z differs from the existing design of the joint and is the crucial phenomenon when designing pot bearing enabling supporting structures. Forced displacement of the structure because off horizontal deviations in the travelling track adds to the forces acting on the gantry. In some cases, this displacement can decrease the acting forces but more important is to be aware of the cases where the effects are summed together.

International standard ISO 12488-1 (Cranes – Tolerances for wheels and travel and traversing tracks –) gives requirements for the track tolerances depending on the total amount of travelling distance in the service life of a crane. Tolerances are divided in to four classes

depending on the total travelling distance. Principle is that if the tolerances of a travelling distance indicated tolerance class are fulfilled, there is no need for proofing the competence of the crane structure. In this study, the selected tolerance class for the tracks was worse than what the expected total travelling distance *L* of the crane in question indicated. (ISO 12488-1 2012, p. 1-4.)

Classification for the tolerance classes and expected total travelling distance for the crane in question are presented in table 4. *L* is calculated using average of measured travelling distance per working cycle (one container from train to stack and travelling back) and total work cycles specified for the crane.

Table 4. Travelling track tolerance classes and total travelling distance (mod. ISO 12488-1 2012, p. 3; Konecranes 2018c; Parviainen 2018).

Travelling distance per working cycle [m] Specified working cycles [pcs] Total travelling distance *L* [km]	50 2 000 000 100 000
Tolerance class	Limits for *L* [km]
1 2 3 4	$50\,000 \leq L$ $10000 \leq L \leq 50\,000$ $L < 10\,000$ Temporary tracks

Readout of the table 4 indicates that for the crane in question, tolerance class 1 should be applied. Instead of the class 1, class 2 was used in the study for fatigue loading, simulating the situation where requirements of appropriate tolerance class are not fulfilled. Increased wear of the rail wheel, other travelling machinery components and travelling track were not studied in detail. This was also the reason why class 3 was not utilized and because its requirements are far from the requirements of the appropriate class 1. Assumption was made that even if the structure would proof its competence in the fatigue loading caused by the excessive deviations in the travelling track, rapid wear of the mentioned components would make class 3 impossible in practice for the required *L*.

In ISO 12488-1 geometrical tolerances for the four tolerance classes have been defined in constructed and operational state. Tolerances for construction are tighter and rails are measured after building or repair work and they only apply for the rails. Operational tolerances

are looser, and they take the rail wheels also into consideration and values are presented as total including the effect of the rail and rail wheels. Operational tolerances consider the variations in the rail measurements and geometry due to wear and possible displacements happening in the crane structure or in the rails. (ISO 12488-1 2012, p. 1, 4.)

Three different tolerance parameters were considered when defining horizontal deviations in the travelling track geometry. First of those parameters was *A* which is the tolerance of span *S*. *A* defines how much the distance between rails can deviate in the whole distance of the track. *Smax* is the maximum value for *S* and *Smin* is the minimum value. Graphical presentation for the tolerance of span is shown in figure 10. (ISO 12488-1 2012, p. 5.)

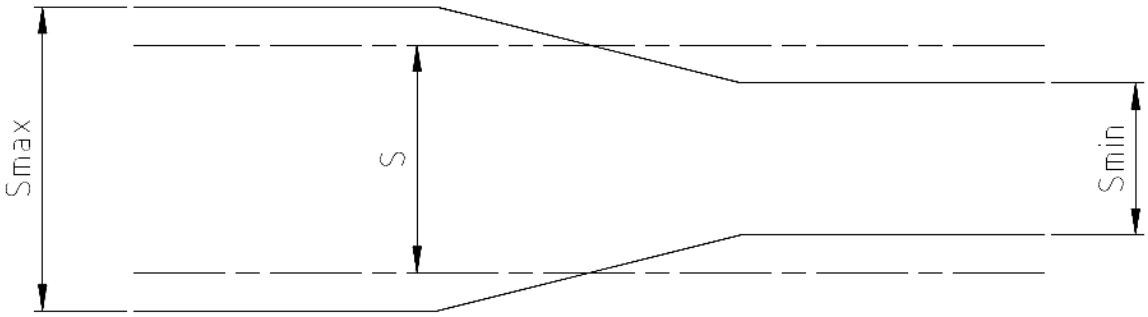

Figure 10. Tolerance of span *S* (mod. ISO 12488-1 2012, p. 5).

Second parameter considered was the tolerance of horizontal straightness *B* which defines how much can any point of single track have offset compared to the theoretical rail line. Third parameter was *b* which is the tolerance of horizontal straightness related to test length of 2000 mm. Graphical presentation of *B* and *b* is shown in figure 11. (ISO 12488-1 2012, p. 5.)

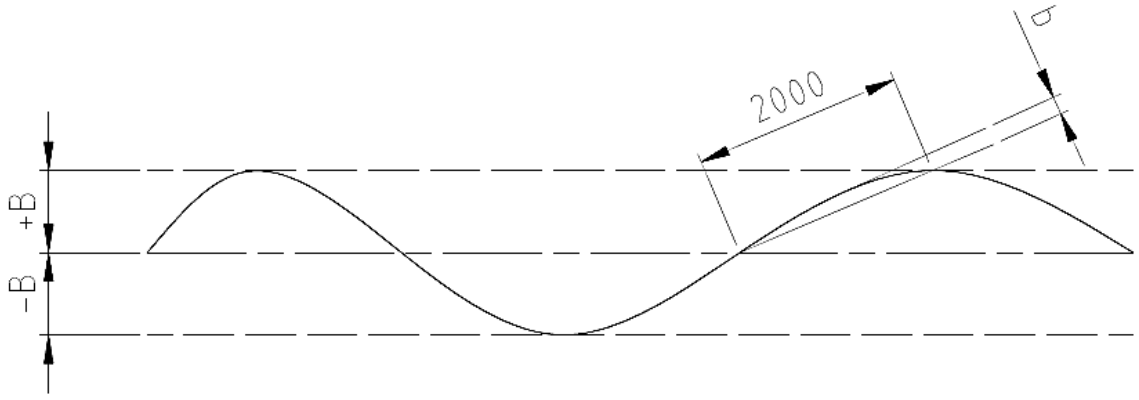

Figure 11. Tolerance of horizontal straightness (mod. ISO 12488-1 2012, p. 5).

Parameter *b* is important addition for *A* and *B* because otherwise the track could have very sharp and sudden changes which would cause additional stress for the bogie structures and components and for the whole steel structure of the gantry. Both *A* and *B* are defined in the construction and operational tolerances, but *b* is only defined in the construction tolerances section of the standard. (ISO 12488-1 2012, p. 5, 17.)

Tolerances used in the determination of the fatigue loading were based on operational tolerances *A* and *B* and on construction tolerance *b.* As a qualitative description of the discussed tolerances it can be said that *A* and *B* are used to define limit values for the rail curve and *b* is used to define average value for the slope of the curve. Tolerances are presented numerically in table 5 for classes 1-3.

Table 5. Tolerances for travelling tracks (ISO 12488-1 2012, p. 5, 17).

Parameter	Tolerance for span S=42.672 [m]		
	Class 1 ±[10+0.25(S-16)]	Class 2 ±[16+0.25(S-16)]	Class 3 ±[25+0.25(S-16)]
A	±16	±22	±31
B	±10	±20	±40
b	1	1	2

Tolerance values in millimetres.

2.7 Static loading

Maximum vertical and horizontal static forces for the lower joint were studied with the help of FEA. Two load combinations were studied, because it was not totally sure which load combination would cause greatest support reaction force. SFS-EN 13001-2 was utilized and thereby regular loads were ignored and only load combinations B and C were studied. Loads and their factors were based on SFS-EN 13001-2, but load combinations were slightly modified. Load combination B was built by modifying combination B3 of the standard by adding occasional skewing according to load combination B5. Load combination C was taken directly as a load combination C9 of the same standard. The mode of failure in the combination C9 was taken as exceptional skewing. (SFS-EN 13001-2 2014, p. 96-99.) In this case the exceptional skewing means a situation where rail wheels on the other track are kept in place with brakes or anti-lifting restraints and travelling machineries on the other rail are working with the maximum moment output. Loading caused by this kind of situation can be described

as failure induced, because it is not possible to happen without any mechanical, electronic or software related failure. Loads and partial safety factors for load combinations are presented in table 6.

Table 6. Loads, load combinations and partial safety factors (Konecranes 2018c; Rautajärvi 2018; SFS-EN 13001-2 2014, p. 96-99).

Loads			Load combination B	Load combination C
Mass of the crane	522 000	[kg]	1.16	1.1
Mass of the hoist load	40 000	[kg]	1.22	1.1
In-service wind	20	[m/s]	1.22	-
Skewing	100	[mm]	1.16	-
Exceptional skewing	250	[kN]	-	1.1

Contraint conditions of the crane are presented in figure 12. Pin joints in the joints of hinged leg and main girders and in the bogies are marked with blue double circles and fixed DOFs are marked with blue arrows. Vertical movement was restricted in every lower joint and movement in rail direction (Z) was restricted in the origo of the coordinate system, on the left side of the gantry. On the rigth side, 100 mm forced displacement was induced to the structure in the case of load combination B. For load combination C, this forced displacement was replaced with horizontal force in the rail direction according to exceptional skewing in table 6. As discussed earlier, the effects of rail deviations were used just in the phase of defining fatigue loading, not in the static case. In the static case it was assumed that all rail wheels would be in centerline of the rail and have 10 mm of gap between rail wheel flange and the rail on both sides of the rail. This constraint was simulated by adding NLS (nonlinear spring) to every lower joint. NLS allows free movement to certain specified point, and after the amount of free dispalcement is reached, linear spring begins to carry load according to its spring constant. Spring constant was defined to be 10^{14} kN/m which is practically rigid with load magnitudes in question. Gap between rail wheel flange and rail side is presented in figure 13.

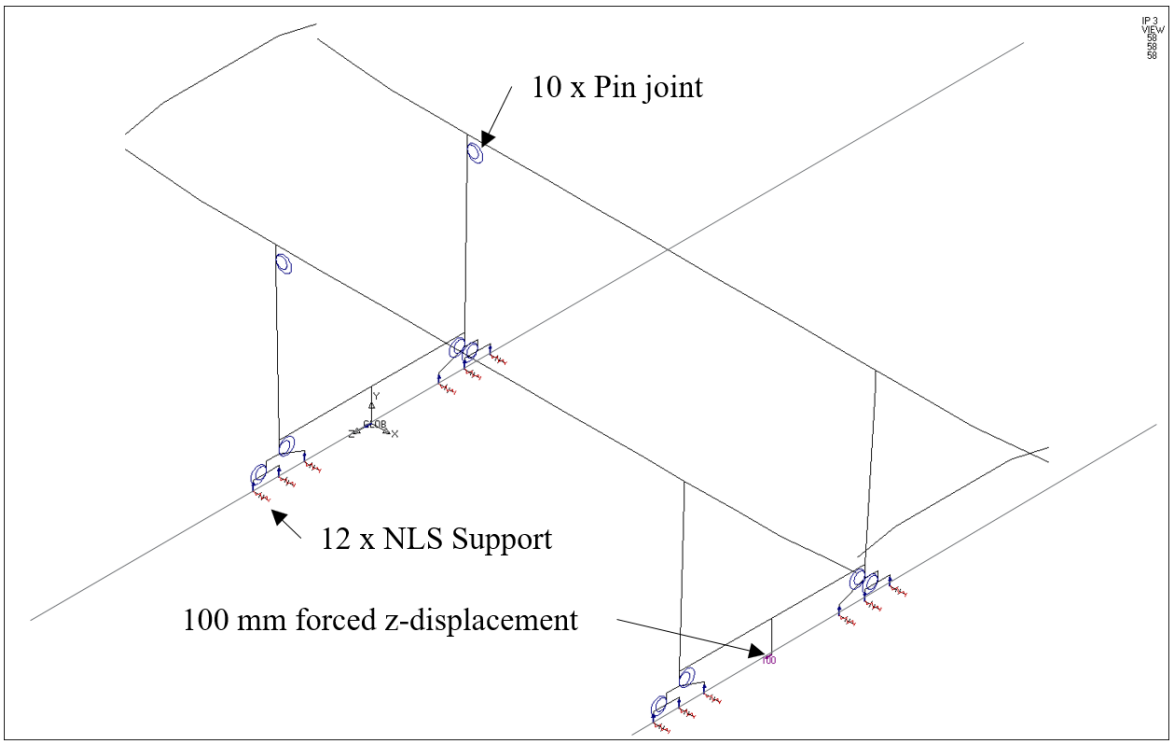

Figure 12. Constraints of the crane.

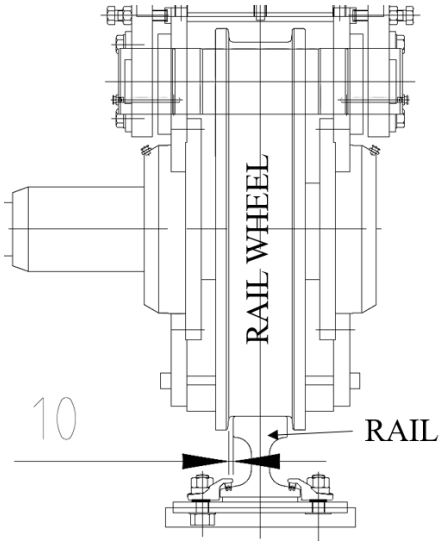

Figure 13. Gap between rail wheel flange and rail side (Konecranes 2018c).

Wind pressure was subjected to the gantry surfaces normal to rail direction because wind acting in that direction, would collapse bogies under the balancing beams without pot bearing supporting external structures. Wind speed wasn't decreased near the ground, but it wasn't applied to the bogie structures. Wind pressure was determined to be 250 N/m^2 according to design wind pressures in SFS-EN 13001-2 (SFS-EN 13001-2 2014, p. 81).

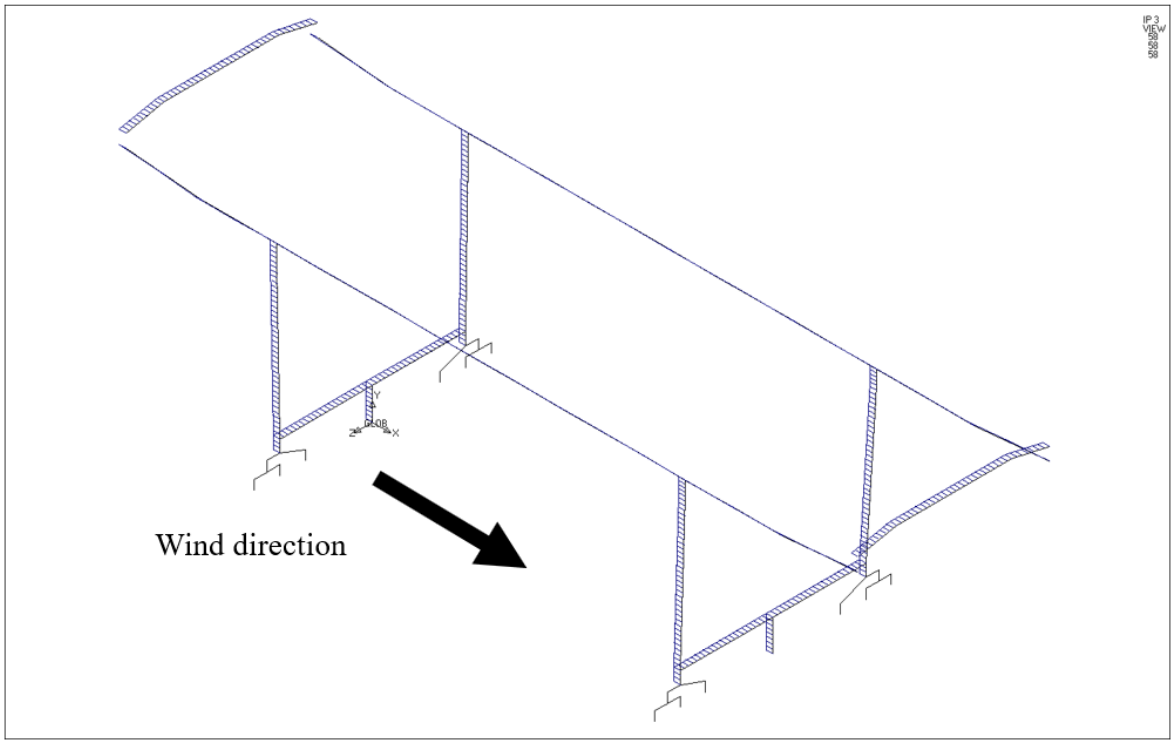

Figure 14. 250N/m^2 in-service wind load for the gantry.

Mass of the gantry was divided equally according to cross-section areas of the steel structure and on point masses presenting masses of machineries and accessories. Mass of trolley as whole and lifted load was subjected to the main girders with vertical point loads presenting wheel loads of trolley wheels. Trolley was located on the side of fixed leg, where the maximum horizontal support force for lower joint was assumed to be. Location of trolley and trolley wheel point loads can be seen in figure 15.

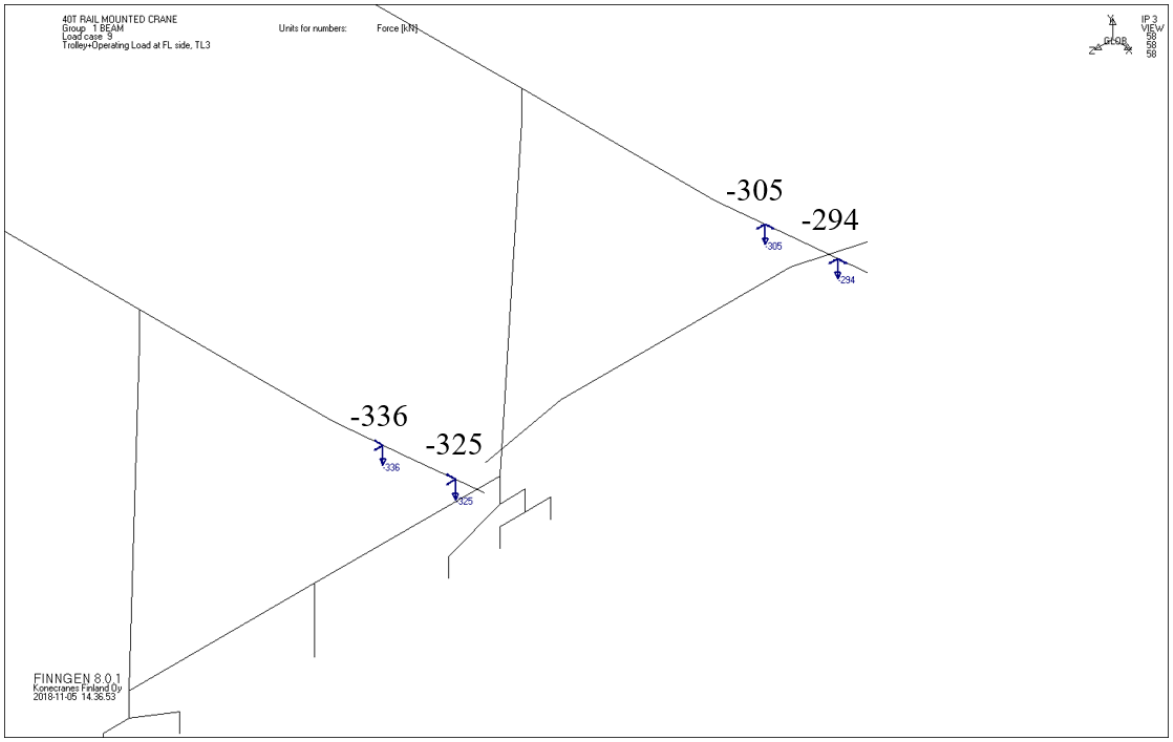

Figure 15. Location of trolley and trolley wheel point loads [kN].

2.8 Fatigue loading

When defining loading history for the lower joint, fluctuation of horizontal force F_x was the variable studied. Justification for ignoring fluctuation of vertical force F_y in loading history determination was the fact that vertical force components would travel just through the pot bearing, not affecting the external support structures in any way and that the fluctuation of vertical loading would be only caused by the location changes of trolley and lifted load. Mass of trolley and lifted load compared to the mass of the gantry are small and thereby changes in the loading levels are also small. If masses, dimensions and pot bearing supporting structures of the crane would be different, fluctuations of the vertical force components should also be studied.

Principle for creating loading history was constant frequent forced displacement in the lower joint with the magnitude specified by combination of travelling track tolerances. If span S is constant in the track length of *cd* (corner distance of the gantry), area restricted by lines drawn from outermost lower joints to each other form a rectangle. Pin joints between hinged legs and main girders should allow values for S beyond the track tolerances without any dramatic load effect for the lower joints while the corners of the crane still form a rectangle.

In the case of fatigue loading, more important is the situation where *S* is changing, and the rectangle is forced to a shape of trapezoid because of the not parallel rails. In this trapezoid state, rotation in the pin joints of hinged legs and main girders are not enough and deformation of the gantry structure occurs. Figure 16 presents the rectangle and *cd*.

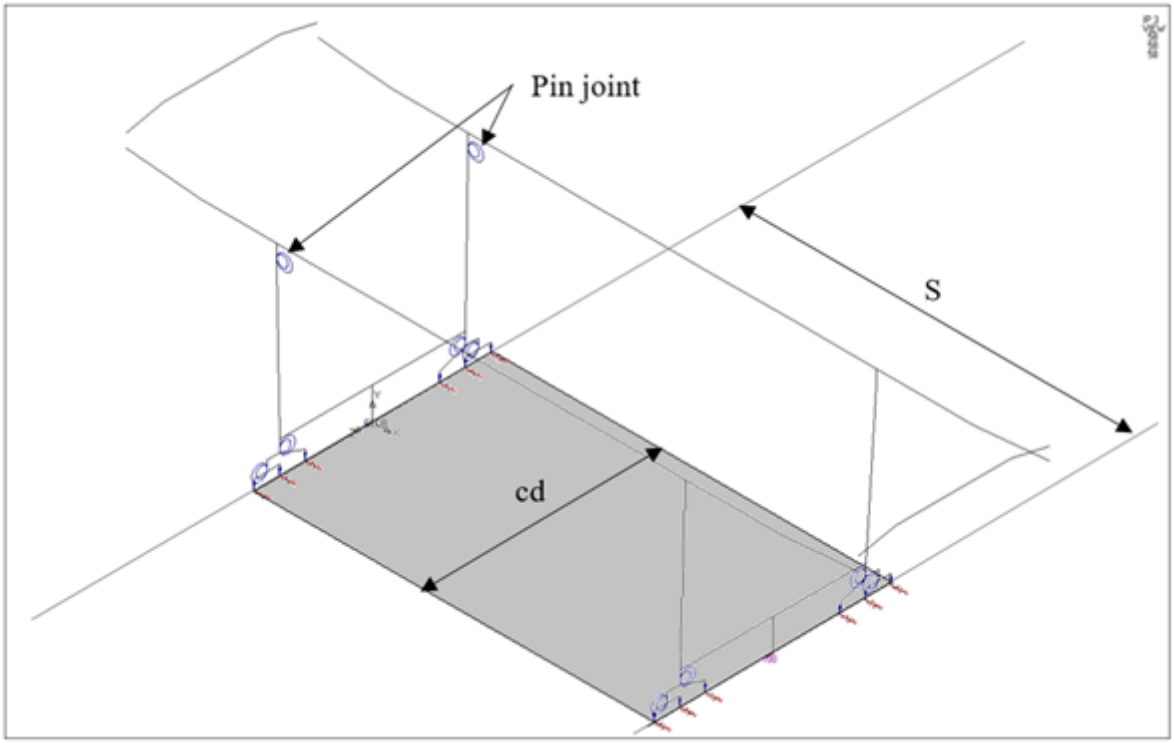

Figure 16. Corner distance *cd* and rectangle formed by crane corners.

Graphical presentation on how travelling track deviations defines the magnitude of forced displacement in the lower joints is shown in figure 17. In this presentation other rail is drawn as straight for the means of simplification of the theory and the other rail has the maximum possible deviations with maximum frequency. Gap between rail wheel flanges and rail sides was not taken into consideration for the sake of simplification and for the fact that when rail geometry is the definitive factor for forced displacement, extra allowed movement would just affect the results in decreasing way and decreasing certainty. Maximum deviations are based on *B* and frequency for the limit values to occur, is based on *b*. Figure is drawn based on track tolerance class 2 which means that 80 meters is the travelling distance required for the rail to get from upper limit to its lower limit and vice versa in the means of *B*.

Because the other rail is straight, all deviations are summed to the deviating rail meaning that numerical values for *B* and *b* are multiplied with two according to the values in table 5. This means that in the case of travelling track tolerance class 2, tolerance of span would be exceeded but as mentioned before, the absolute value of the span is not that relevant in the means of fatigue study of the lower joint. Squares in the figure 17 present the outermost bogies numbered with 1 and 2, *e* is the rail wheel line offset between the outermost bogies and *Z* is travelling distance.

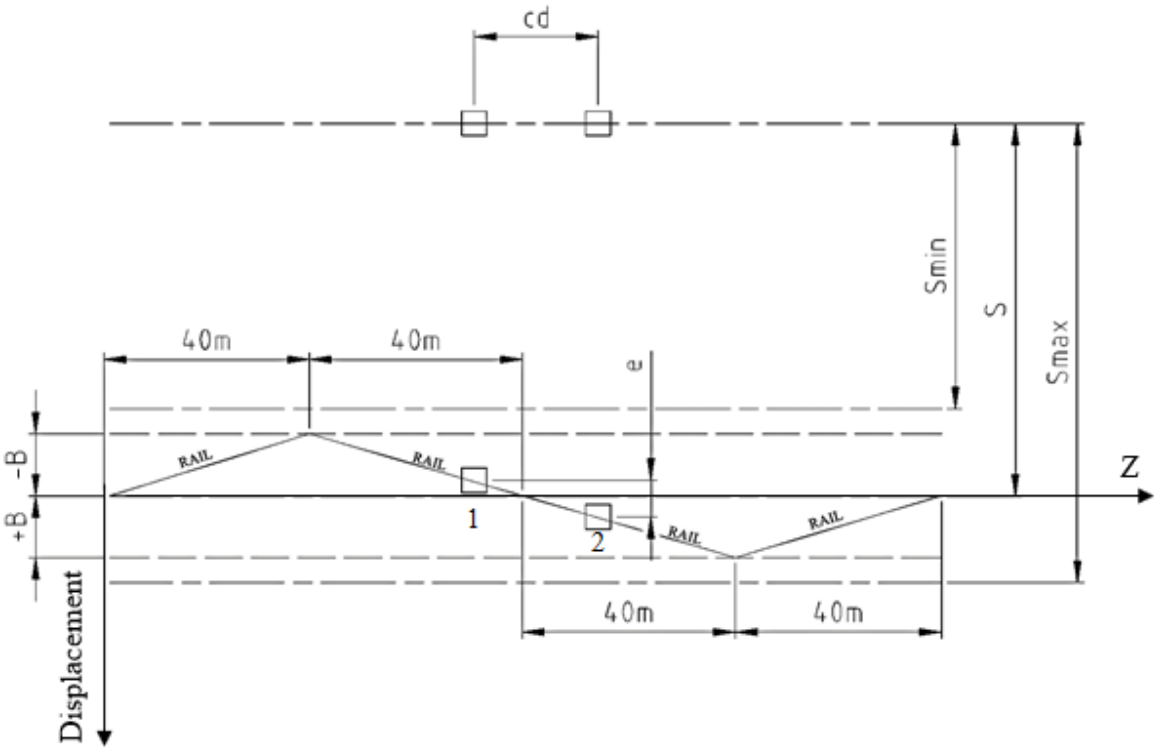

Figure 17. Graphical presentation of displacements forced by deviations of travelling track.

One travelling working cycle was defined to be 160 m according to figure 17. Bogie number 2 was used as a reference point which was subjected to travel the distance according to working cycle followed by bogie number 1. Parameters for bogie displacement- and Z coordinates definition and the coordinates themselves are presented in table 7. Five different locations were determined for the crane to fulfil one travelling working cycle. This travelling working cycle was then compared to the average travelling distance per one container (working cycle) to obtain amount of load changes during specified service life of the crane.

Table 7. Parameters and values for bogie displacement- and Z-coordinates.

Length	40000	[mm]
B	40	[mm]
Slope	1	[mm/m]
cd	25240	[mm]
e	25.24	[mm]
Z [m]	Displacement 1 [mm]	Displacement 2 [mm]
0	25.24	0
40	-14.76	-40
80	-25.24	0
120	14.76	40
160	25.24	0

Constraints for FEA-model of forced displacement were subjected to the gantry same way in every coordinate location, only changing the values of the displacement. Horizontal supports in X-direction were placed to the outermost bogies on the hinged leg side. Horizontal supports in Z-direction were placed on both sides, middle of sill beams. Vertical supports were added to every lower joint and forced displacement to the outermost bogies of fixed leg according to table 7. Constraints and forced displacements are presented in figure 18.

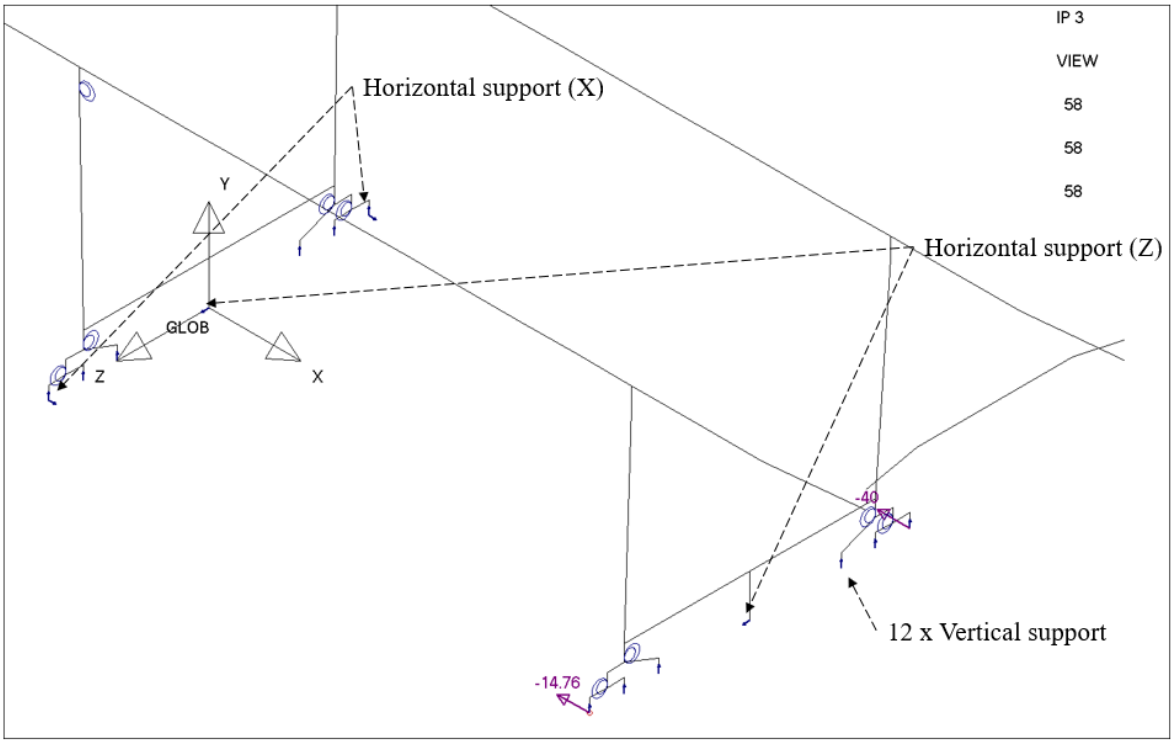

Figure 18. Constraints and displacements for bogie 2 Z-coordinate 40 m.

2.9 Design forces

Results of static analysis for the horizontal force F_x can be seen in figure 19 for both loading combinations B and C. Combination C resulted greater forces than combination B. Results for vertical force F_y are presented in appendix I.

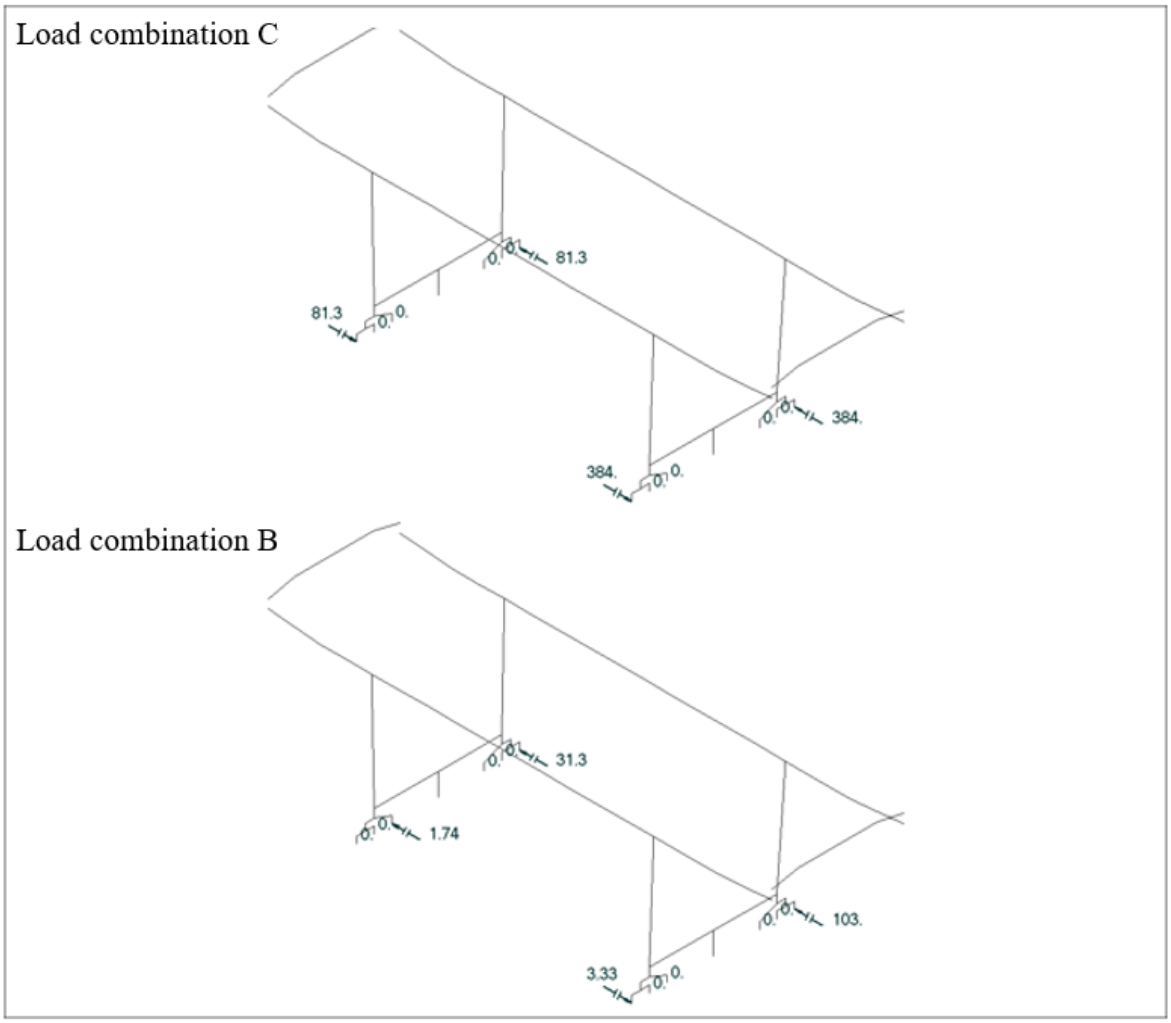

Figure 19. Results of F_x in load combinations B and C.

Loading history for travelling distance of 320 m is presented graphically in figure 20. In the scope of the gantry dimensions and displacements set, it can be said that factors affecting to horizontal load are wheel line offset *e*, and sign of the span. Magnitude of span deviation isn't affecting in these dimensions, but the direction of the span deviation is. Differences in absolute values of horizontal load depending on the direction span deviation. More force is required to stretch the span wider than to compress in narrower. This is most probably dependent on the fact, that middle line of fixed leg is tilted outwards 3 degrees meaning that

stretching the span also lifts the side of the gantry upwards while gravity is acting against the movement. Compression brings the structure downwards, meaning that mass on top the fixed legs is helping in the deformation.

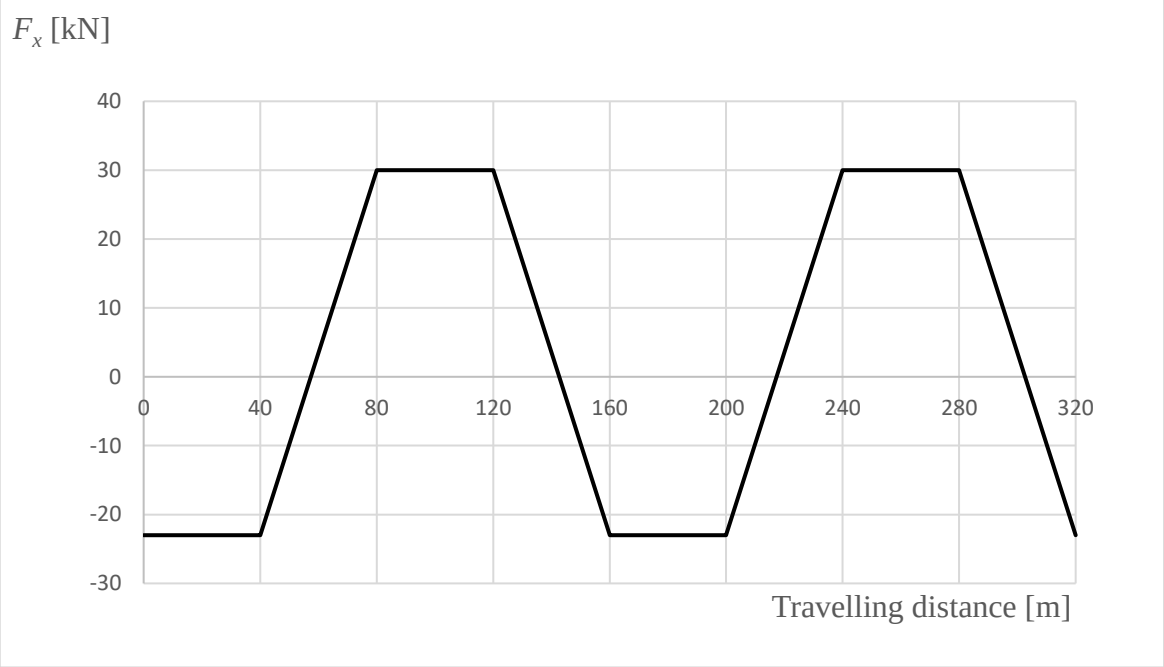

Figure 20. Loading history of F_x over sample distance of 320 m.

Numerical data for both static and fatigue loading is presented in table 8. Fatigue loading data was kept unprocessed in this phase and values from this table were utilized in the design phase according to requirements and constraints of a single design solution.

Table 8. Numerical data for static and fatigue loading used in design phase.

Static loading	B	C	**Fatigue loading**									
Max F_x [kN]	103	384	Z [m]	0	40	80	120	160	200	240	280	320
Max F_y [kN]	932	877	F_x [kN]	-23	-23	30	30	-23	-23	30	30	-23

3 CONCEPTUAL DESIGN

First step of design work was conceptual design where a working concept was created. Pot bearing solution with matching DOF requirements was not found and existing structures and solutions couldn't be applied. Konecranes and other crane manufacturers have solutions for lower bogie joints with matching DOFs, designed for greater rotations for the purposes of curved tracks. Generally, these joints utilize pin joints in direction of two axes allowing desired rotations and would theoretically work with straight tracks with tolerance issues. Motivation for developing totally new pot bearing solution for lower bogie joint was much greater than further development of the curved track bogie joint and that is why curved track bogie joints with pin joints were scoped out from this thesis. Workflow of conceptual design was based on systematic product development process theory, introduced first time in 1977 by Gerhard Pahl and Wolfgang Beitz. (Pahl et al. 2007.) Step-by-step following of the theory in question wasn't carried out, but workflow used was an adapted version, better suitable for the problem in question. Several possible variants for the lower joint were created and then evaluated with technical-economical approach to find the best solution for further and detailed development. Pot bearing lower joint was focused and design process handled the structures which enable the use of the bearing.

3.1 Design process

Trimmed and applied version of the systematic product development process is presented in figure 21. The original flowchart contains three more steps listed below with the right locations on the flowchart (Pahl et al. 2007, p. 160):

- "Establish function structures" (after abstract)
- "Combine working principles into working structures" (after working principles)
- "Select suitable combinations" (after combining working principles into working structures)

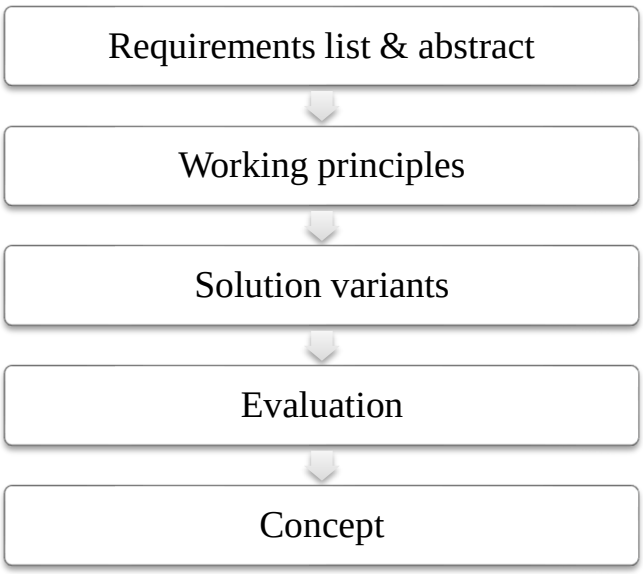

Figure 21. Workflow of conceptual design (mod. Pahl et al. 2007, p. 160).

3.2 Requirement list & abstract

To be able start the conceptual design process, requirements list must be done. Requirement list is a result of task clarification and first part of conceptual design and it consist of demands and wishes specified for the product. Performance of the final product must fulfil the demands section but wishes can be neglected for a good reason. When demands are fulfilled, the system, machine or component works in a way specified by the customer. Fulfilling wishes can decrease operating costs, make the use of the product in question easier or increase attractiveness of the product in the eyes of a customer, making the product more interesting. Requirements are divided into quantitative and qualitative sections, from which the qualitative ones should be refined to be quantitative by giving numerical values for a phenomenon if the nature of the phenomenon and usable resources enables it. (Pahl et al. 2007, p. 145-153.)

For the supporting structures of pot bearing, requirement list presented in table 9 was created. Dimensional requirements were based on spatial restrictions of the bogie configuration and operational environment. Supporting structures had to fit between motors and transmissions and not to widen bogie and balancing beam assembly too much. Force requirements were based directly to previous calculations both in static and fatigue loading cases. Operational requirements were specified to fulfil DOFs in the way desired. Assembly and maintenance requirements were kept simple, just to ensure the possibility for wearing parts change and

for easy detaching of bogie from balancing beam. If detaching can be done only by z-directional movement, excessive lifting of any component or structure is avoided by rolling the bogie out under the balancing beam end. This way safety and stability aspects can be met much more easily. All the requirements weren't transformed into quantitative form because of lack of information. "Low resistance against allowed rotations" was treated as qualitative measure because the exact threshold value for rotation resisting force or moment couldn't be known before testing of the newly designed lower joint configuration. Assembly and maintenance related requirements were handled with binary yes or no answers because describing them accurate numerically would have been impossible. Fixed measurements exist for motors, transmissions and transmission support and supporting structures interference with those could be numerically presented, but it was also treated as binary because of simplicity of the table.

Table 9. Requirements list for pot bearing supporting structure.

Demand/Wish	Requirements
	- Dimensions:
D	600 mm maximum offset from rail line in x-direction
D	100 mm distance from yard level
W	No interference: motors, transmissions or transmission moment support
	- Forces:
D	384 kN maximum static horizontal force capacity
D	Capacity against specified fatigue loading
	- Operation:
D	2 ˚ rotation capacity around x- and y-axis
D	0 ˚ rotation due to horizontal load around z-axis
W	Low resistance against allowed rotations
	- Assembly & maintenance
D	Mechanically connected wearing components
W	Structure allows detaching of bogie only with z-direction movement

After requirement list had been gathered, abstraction was carried out. In this context abstraction means converting the content of requirement list eventually to simple, clear and solution neutral qualitative definition of the problem which is handled. In the phase on requirement

list drafting, measures were intentionally given numerical values to specify accurate requirements. In abstraction phase, these requirements are converted back to qualitative. Intention of abstraction is that all connections, links and mindsets which the designer or designers might have in their minds to some preliminary or conventional solution, would be broken maximizing probability to achieve the best possible solution to a problem in question. Workflow of abstraction starts from deleting of wishes and operationally not crucial demands from the requirements. Assembly and maintenance related requirements and all additional wishes were deleted in this phase. Next step was to convert crucial demands into qualitative information and generalizing them. (Pahl et al. 2007, p. 161-165.) Results of abstraction after this step are the following:

- Rotation around z-axis restricted
- Free rotation around x- and y-axis
- Practically free geometry inside certain limits

Force and fatigue capacity related requirements were included in the rotation aspects because support reactions due to the horizontal force F_x are the only thing preventing the bogie collapsing under the balancing beam, keeping the z-rotation practically zero. In other words, force bearing capacity isn't relevant, but it is inevitable when certain natural displacement caused rotation must be restricted. Values for geometry of the components are strict but they still leave room to work with. That is the reason why geometry was thought to be practically free with certain limitations.

Final step of the abstraction was to present the previous steps in a problem form sentence without referencing to any solution in any way (Pahl et al. 2007, p. 165). Result of the final step of abstraction for the pot bearing supporting structure was: Block rotation around z-axis while allowing rotation around x- and y- axis staying inside specified primary dimensions.

Next step of systematic product development process would be to establish function structures. This means that whole operation of a system is described as function, which is then divided into smaller sub functions, whose working combination will fulfil the function. (Pahl et al. 2007, p. 169-171, 178.) In this development process where supporting structures of pot bearing being in the scope, supporting structures were considered as one sub function. Overall function consisting of bogies and balancing beams were initially defined to remain the

same so development work was focused just on one sub function, the supporting structures of pot bearing.

3.3 Working principles

According to Pahl and his co-writers (2007, p 181): “Working principles need to be found for the various subfunctions, and these principles must eventually be combined into a working structure.”. Three different principles were found to fulfil the requirement expression, formed in the final stage of abstraction. In addition to these three, other principles were also discovered in the first stages of drafting, but they revealed to be fundamentally uncertain in the terms of the requirements. Some of these freshly rejected ideas gave properties to the presented working principle ideas and were that way involved and considered in the whole design process. Phase of combining the sub function fulfilling working principles into working structures and selecting the suitable ones was executed already in the phase of searching the principles, because once again, only the supporting structures were studied and therefore working principle presents also the working structure and combinations don’t exist (Pahl et al. 2007, p. 181-186). Schematic presentations of the working principles were created by using Siemens NX 10 3D CAD-software (computer aided design). Dimensions and shapes of the structures and components are rough and not adaptable directly. Figures are just presenting the principles.

Pot bearing with side supports and uplift restrictors was the first idea to solve the problem. In this principle, pot bearing carries all vertical force and collapsing of bogie frame under the balancing beam is prevented with compressive force in side supports. Between side supports of bogie and balancing beam, there are sliding members, allowing y-rotation by relative sliding against each other. In this stage requirement of preventing z-rotation and allowing y-rotation are already fulfilled. To enable also x-rotation, the sliding members have slightly convex contacting surfaces. Principle is presented in figure 22.

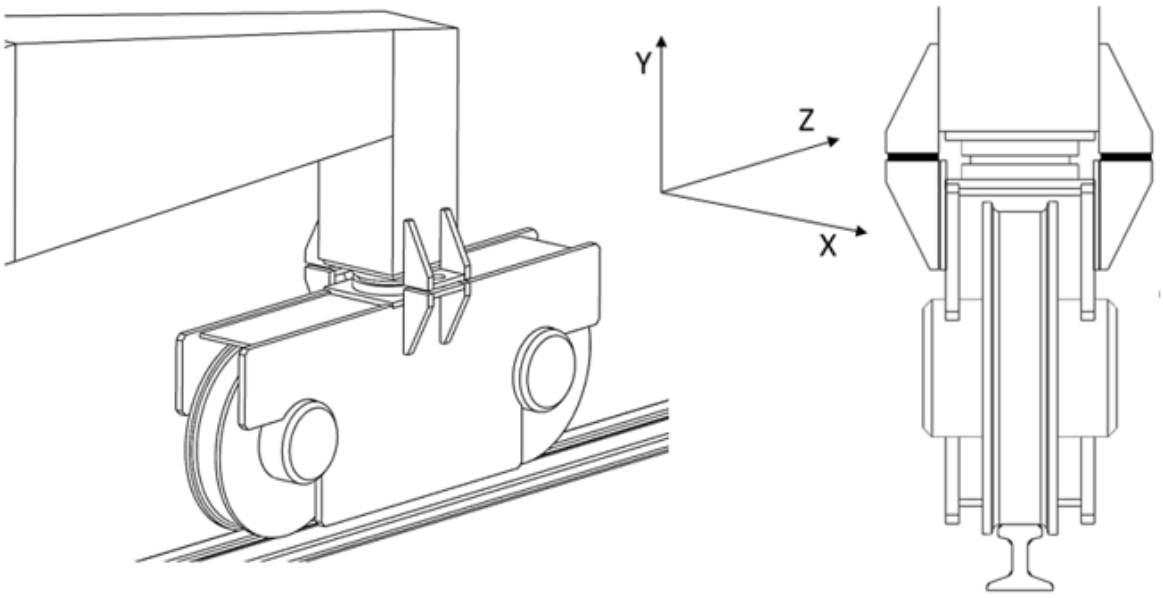

Figure 22. Side supports and uplift restrictors.

Sliding material was preliminary selected to be some high preforming polymer of softer metallic material compared to steel, preventing wear and deformation of the structural components. If F_x is too great, it is possible that uplift will happen in the pot bearing, changing the tilting point from center of pot bearing to the side support on compression side. Possibility of this phenomenon requires uplift restrictors added to the structure. In ideal state of the bogie and balancing beam assembly, horizontal force is virtually zero, and no vertical force is travelling through the side supports and small gap between sliding members could be achieved, thereby not restricting the y-rotation in any way. In practice this kind of situation is impossible and most probably bogie would lean on other side, causing permanent contact between sliding members, inducing rapid wear and friction restricted y-rotation.

Second working principle drafted, was pot bearing with external support rods. In this principle, support reaction moment M_z is generated by compression, tension or their combination in the support rods. This way z-rotation is prevented. Rotation around x- axis is allowed by spherical joints in upper ends of the support rods placed in a way that x-directional rotation axis of the pot bearing is in line with the rotation center of spherical joint. This way x-rotation can be achieved without support rods restricting the rotation by enforced stretching or compressing of the rods. By adding spherical joint also to the lower end of supporting rods, y-

rotation can be achieved by inclining the support rods slightly. Second principle is presented in figure 23.

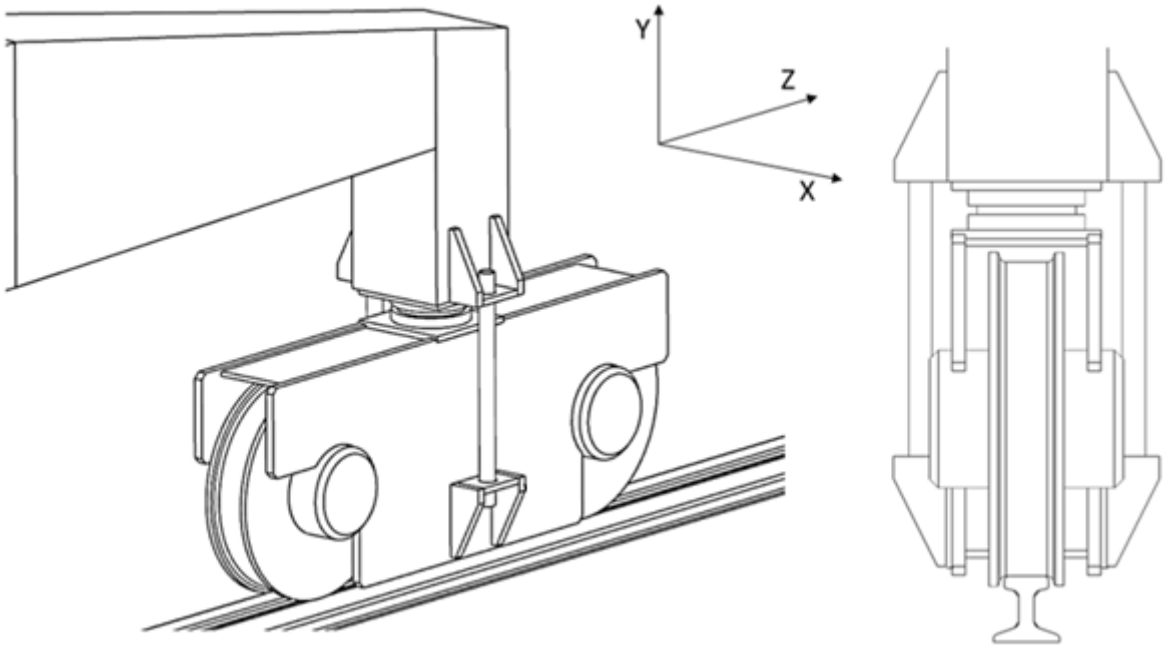

Figure 23. External support rods.

This inclination of the rods restricts the y-rotation because the rods are subjected to stretching. This enforced stretching of the rods was preliminary considered to be very low, causing small scale tension to the rods. This tension is in fact lowered if the compression of elastomeric disc of pot bearing is taken into consideration. Support rods cannot provide great magnitude rotation for the joint, but in the required small-scale rotation, kinematics of the joint would be sufficient.

For third working principle, fork support was drafted. This principle is presented in figure 24. Idea in the fork support is that bending resistance of the fork plates prevents z-rotation of bogie. Sliding of fork plates against sides of bogie frame, enable x-rotation. The actual siding happens between separates sliding member, which are fixed to the mentioned components. By keeping the fork plates surface of contact narrow in z-direction, y-rotation can be achieved. This requires small gap between the sliding members, but the narrowness of the sliding contact surface enables required y-rotation with very small-scale gap.

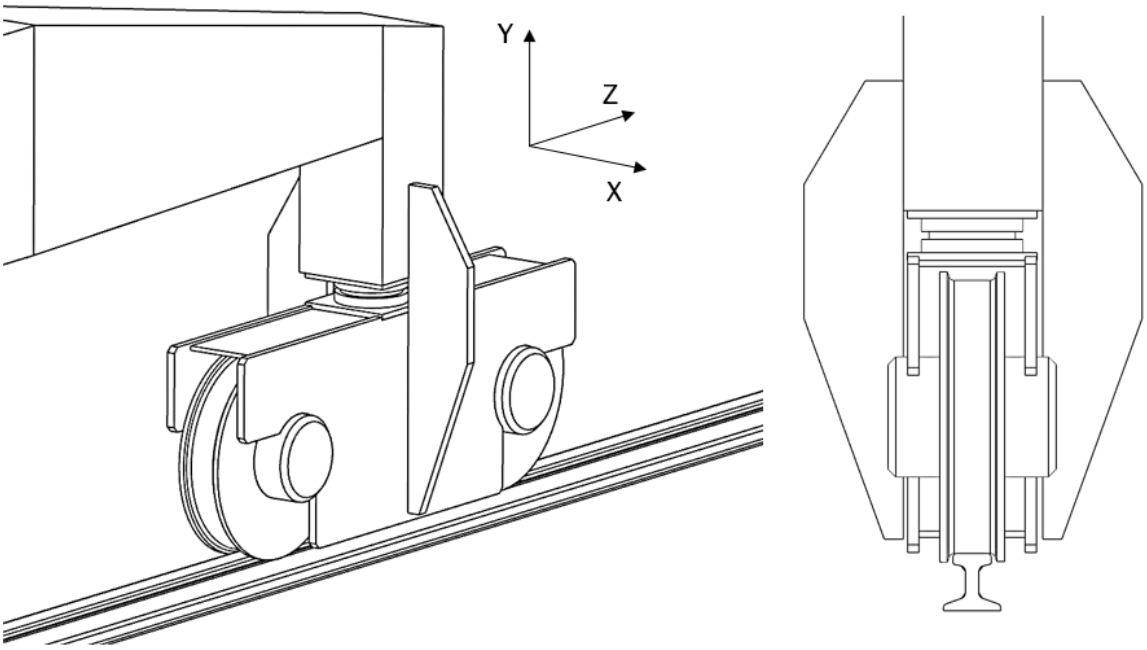

Figure 24. Fork support.

Principle of fork bearing can be also flipped upside down, when fork plates would be fixed to the bogie frame, and sliding would happen against the balancing beam sides. Fork plates can also be beams or other more complex structures, but the presentation is drawn with plates on their edges just to promote the narrow contacting surface of supports and bogie frame. This principle has the same basis than in the second principle because this kind of joint configuration cannot provide possibility for great magnitude y-rotation but in the required measures, fork support could be a sufficient solution.

3.4 Solution variants

Working principles presented were used when solution variants for the concept were created. These solutions variants were evaluated against each other later. To get the most truthful result from the evaluation, concretization of the principles is needed, and this is performed by preliminary calculations and creating layouts according to the principles (Pahl et al. 2007, p. 190-191). Calculations were based on standard SFS-EN 13301-3-1 and for additional information related on fatigue, Eurocode 3 SFS-EN 1993-1-9 standard was utilized. Design and calculations were focused on the supporting structures and bogie frame was considered to have adequate strength and stiffness due to great plate thicknesses and was left out from the calculations.

Solution variants 1 and 2 are based on the principle of external support rods and variants 3 and 4 are adapted from the fork support principle. Against the theories of systematic development procedure, first principle was neglected already in this stage because of the previously mentioned leaning problem. Leaning problem was considered so challenging to handle, that development was focused on the other two principles.

3.4.1 Variant 1

Idea in the variant 1 is that the supporting rods on both sides of the bogie generates supporting moment around tilting point of pot bearing by compression and tension. Sign of the loading is dependent on the direction of F_x meaning that loading direction alternates in both rods. Spherical joints according to related principle were constructed with convex spherical caps and their concave pair manufactured from high performance polymer or metallic material(s) with lowest possible friction coefficient between spherical caps. Assembling the construction, bolted connection in the direction of the rod was selected, because then spherical joints could be tightened with simple tools. In this variant threaded bar is used to carry loading in tension and round tube placed around the threaded bar is used to carry compressive loading. In this configuration where the loading is always divided to two members, loading levels can be maintained twice as low than with just using one tension member per side. Assumption was made that the spherical caps can slide against each other virtually with no friction, enabling loading in the rods in pure axial direction without constraining moment. Fixing the joint points to sides of bogie frame and end of balancing beam is drawn very simple, focus being on the rod arrangement. Drafted layout of variant 1 is presented in figure 25.

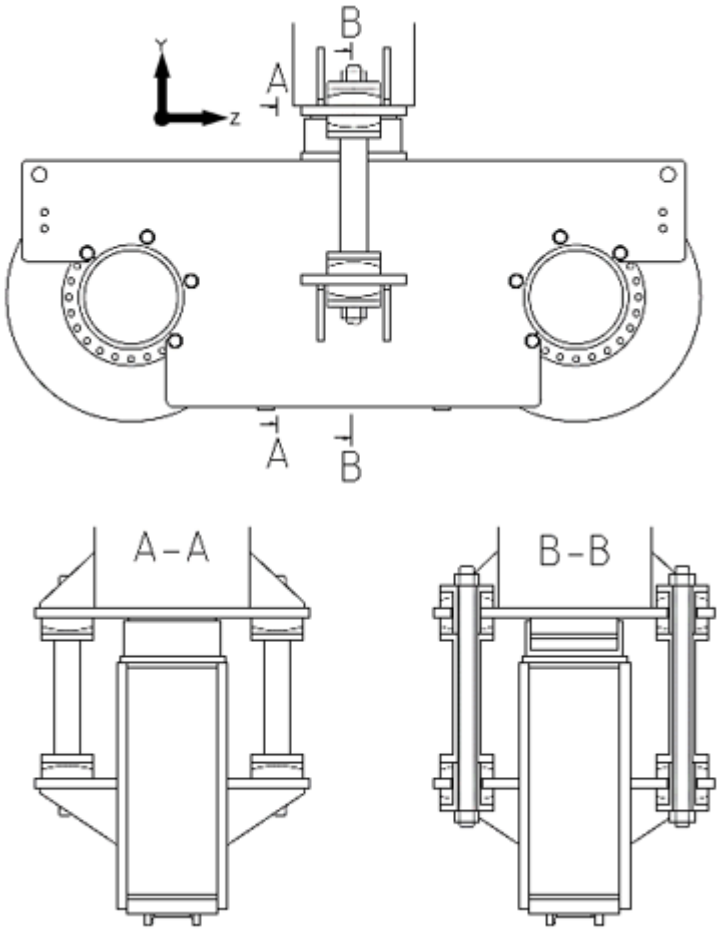

Figure 25. Variant 1.

Things that were checked in this phase to ensure preliminary competence of the structures were the following:

- Axial capacity of the threaded bar
- Buckling capacity of the round tube
- Fatigue loading capacity of the threaded bar
- Fatigue loading capacity of the welded joints of round tube.

Fatigue loading of threaded components isn't initially a good thing because of the large number of notches in the bottoms of the threads and that is why fatigue is the dimensioning measure of the threaded bar. To achieve acceptable buckling capacity, the round bars requires such a great cross-section area compared to pure axial capacity that stress levels maintain low in general and especially in the fatigue loading. Because of low normal stresses in the tube, welds of the tube should have enough capacity because of low amplitude fatigue loading.

Figure 26 presents just the loads keeping the bogie not rotating around the tilting point and collapsing under balancing beam. Rod forces F_{rod} tend to rotate the bogie to counter clockwise and F_x tries to rotate it clockwise. Equilibrium of M_z defines F_{rod} when F_x is already know based on the definition of loading. Moment arm for both F_{rod} is r_2 and r_1 for F_x.

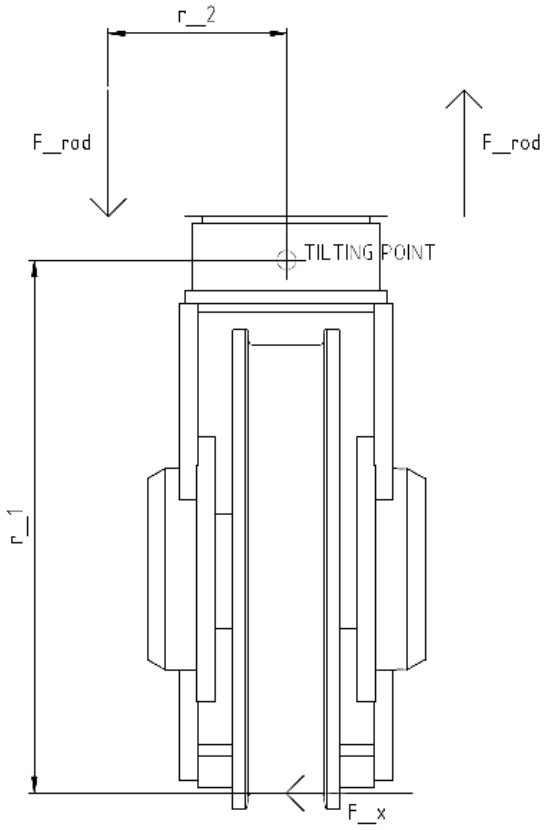

Figure 26. Simplified force diagram of lower joint for solution variant 1.

Buckling being the most probable dimensioning measure of the compression round tubes and fatigue being the most probable dimensioning measure of threaded bars, sufficient A_{rod} (cross-section area of rods) was calculated for checking purposes for both round tube and threaded bars. A_{rod} can be calculated with the following equation for both members:

$$A_{rod} = \frac{F_{rod}\gamma_m}{f_{y\_rod}} \quad (1)$$

In equation 1 γ_m is resistance coefficient and f_{y_rod} is yield stress of the rod material. Value for γ_m is 1.1 when limit state method is used to proof competence of a structure according to SFS-EN 13001-1. Individual loads were multiplied by partial safety factors when defining

loading, so in addition to those safety factors, extra certainty is gained by using γ_m when calculating stresses. (SFS-EN 13001-1 2015, p. 43-44.) In the case of threaded bar, A_{rod} is the actual stress area, taking into consideration the varying thickness of the bar due to threads.

In the case of buckling of round tube, limiting compressive design force N_{Rd_t} can be calculated with following equation (mod. SFS-EN 13001-3-1 2018, p. 54):

$$N_{Rd\_t} = \frac{\kappa f_{y\_t} A_t}{\gamma_m} \tag{2}$$

In equation 2, κ is reduction factor, f_{y_t} is yield strength of round tube material and A_t is the cross-section area (SFS-EN 13001-3-1 2018, p. 54). To be able to obtain κ, following equation must be utilized (SFS-EN 13001-3-1 2018, p. 54):

$$\kappa = \frac{1}{\xi + \sqrt{\xi^2 - \lambda^2}} \tag{3}$$

In equation 3, λ is slenderness which is a measure to describe buckling capacity against cross-section area and ξ is auxiliary variable which can be calculated with the following equation (mod. SFS-EN 13001-3-1 2018, p. 54):

$$\xi = 0.5[1 + \alpha_t(\lambda - 0.2) + \lambda^2] \tag{4}$$

In equation 4, α_t is parameter describing imperfections of the tube and it is dependent on the type of cross-section. Manufacturing method, welding, cold forming or hot rolling and dimensional proportions affect α_t. For circular hot rolled hollow sections in structural steels under yield strength of 460 MPa, α_t is 0.21. (SFS-EN 13001-3-1 2018, p. 56.) Slenderness λ in equations 3 and 4 is calculated based on Euler's critical buckling capacity and can be calculated with following equation (mod. SFS-EN 13001-3-1 2018, p. 54):

$$\lambda = \sqrt{\frac{f_{y\_t} A_t}{N_{k\_t}}} \tag{5}$$

In equation 5, N_{k_t} is the Euler's critical buckling capacity. Figure 27 presents graphically constraint conditions of the Euler case and buckling form. Spherical caps are simplified to form of pin joints. (SFS-EN 13001-3-1 2018, p. 52-54.)

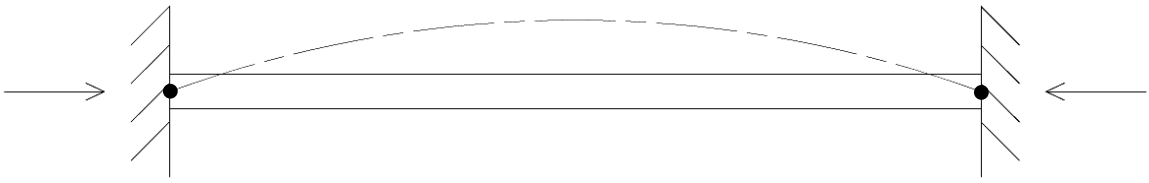

Figure 27. Constraint conditions and buckling form (mod. SFS-EN 13001-3-1 2018, p. 53).

N_{k_t} in equation 5 for the presented constraint condition is calculated by the following equation (mod. SFS-EN 13001-3-1 2018, p. 53):

$$N_{k\_t} = \frac{\pi^2 E I_{tube}}{{L_t}^2} \tag{6}$$

In equation 6, E is elastic modulus, I_{tube} is moment of inertia of the cross-section of round tube and L_t is length of the round tube or compression member in general. Buckling calculation procedure takes into consideration manufacturing imperfections induced geometrical imperfections, which reduce the allowable compressive force compared to the ideal elastic situation, described by Euler's buckling. More complex buckling phenomena were not included to the preliminary dimensioning calculations. (SFS-EN 13001-3-1 2018, p. 52.)

Calculation of fatigue loading capacity for both round tubes and threaded bars was based on theory of constant amplitude loading according to the loading history determined earlier. Fatigue loading capacity can be presented generally with Wöhler-curve. It is a log-log presentation where stress level range $\Delta\sigma$ is on vertical axis, and number of cycles N is on horizontal axis. The curve has knee point (5 million cycles), which defines fatigue limit for $\Delta\sigma$. If $\Delta\sigma$ stays under the fatigue limit for purposes of simplification an assumption can be made that the component could theoretically go through infinite amount of load changes without damages. If $\Delta\sigma$ is higher on the scale, service life of the component is dependent on the amplitude of $\Delta\sigma$ in power of three. These curves have been produced experimentally for different kind of joint geometries and they have been set in way that 97.7 percent of the

tested components survive the required amount of load changes, meaning that in most cases in-built safety of the curves is excessive. The curves for different joint geometries have been classified according to characteristic fatigue strength $\Delta\sigma_c$ which leads to 2 million cycle service life. (Niemi 2003, p. 95-97; SFS-EN 13001-3-1 2018, p. 48-49; SFS-EN 1993-1-9 2005, p. 13-17.) Experimental testing of the newly designed product should be utilized to ensure adequate fatigue life of a component or structure. Example of Wöhler-curve is presented in figure 28.

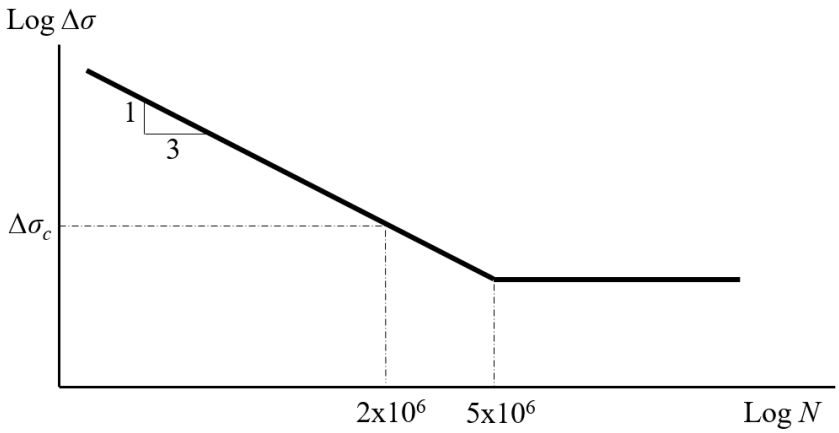

Figure 28. Wöhler-curve (mod. Niemi 2003, p. 95).

SFS-EN 13001-3-1 crane standard is based on the same principles than Eurocode 3 and what Niemi (2003) has presented. SFS-EN 13001-3-1 presents the same matter in more complex form with several auxiliary equations and parametrized tables. Results are still the same than calculated with the guidelines of other mentioned references. Because of unnecessary complexity of SFS-EN 13001-3-1 relating to fatigue calculation, fatigue calculations were based on equation of Niemi (2003) with the exception that symbols were changed according to crane standard. In other words, presentation of crane standard was clarified to much more clearer form. Cycles during service life N_t can be calculated with the following equation (mod. Niemi 2003, s. 96; SFS-EN 13001-3-1 2018. p. 45-49):

$$N_t = \left(\frac{\Delta\sigma_c}{\gamma_{mf}\Delta\sigma_{Rd}}\right)^3 \cdot 2 \cdot 10^6 \quad (7)$$

In equation 7, $\Delta\sigma_c$ is characteristic fatigue strength for a specified joint geometry, $\Delta\sigma_{Rd}$ is limit design stress range and γ_{mf} is fatigue strength specific resistance factor. N_t can be obtained from the loading history and values for $\Delta\sigma_c$ are specified in SFS-EN 13001-3-1. Values for $\Delta\sigma_c$ can be obtained also from Eurocode 3 and other references, but values presented in crane specified standard were considered the most suitable for purposes of crane component design.

When considering safety factor for fatigue, two separate issues must be considered. The easiness of crack detection and consequences of possible failure. Consequences criteria is divided into two sections: Fail-safe and non-fail-safe details. Non-fail-safe details are further divided to two sections from which other is hazardous for persons and the other is not. Easiness of crack detection is divided to three categories dependent on is it possible to check the detail for possible fatigue cracks with or without disassembly or is it non-accessible. (SFS-EN 13001-3-1 2018, p. 41.) Inspecting threaded bar in variant 1 requires disassembly of the components but it can be classified to fail-safe detail because according to SFS-EN 13001-3-1 (2018, p. 41): “Fail-safe structural details are those, where fatigue cracks do not lead to global failure of the crane or dropping of the load.”. Lower joint of a bogie assembly was considered fail-safe on this basis. With these boundary conditions γ_{mf}, for fail-safe detail, accessible with disassembling, was specified to be 1.05 (SFS-EN 13001-3-1 2018, p. 41).

Justification for using long threaded bars in tension members was that by lengthening the threaded bars and preloading them against the round tubes, stiffness of the bars could be lowered and because of that fatigue loading subjected to the bars also lowered. By doing this, threaded bars with initially poor fatigue properties were adapted to fulfil requirements of the application. (SFS-EN 13001-3-1 2018, p. 27-30, 98-100.)

Calculations for static equilibrium and competence proofing of components for solution variant 1 are presented in appendix II.

3.4.2 Variant 2

At first sight solution variant 2 presented in figure 29 seems almost identical compared to variant 1 and could therefore just be an optional layout for variant 1. Differences in variant 2 are that long threaded bars are replaced with shorter and separate screws in both ends of

the support rods and round tube is replaced with hot rolled, cold formed or welded U-profile. In addition to these changes the main difference compared to variant 1 lays in the basic principle of handling F_x induced M_z. In variant 2, under collapsing of the bogie is prevented just by compressive force in one U-profile at a time. Screws in the ends of U-profiles act as a safety measure in a situation where F_x is so great, that bogie would start to rotate around z-axis, around the tilting point. In this situation tension in the screws would prevent the collapsing. Screws also keep the profiles in their right positions in normal operation. Reason for this kind of configuration was that by doing so, the possible fatigue related problems of the threaded components could be avoided by using them just in the extreme static cases. Because normal operation of the components is limited just to compression of U-profiles, spherical caps, similar than in solution 1, are placed just on the ends of the profiles.

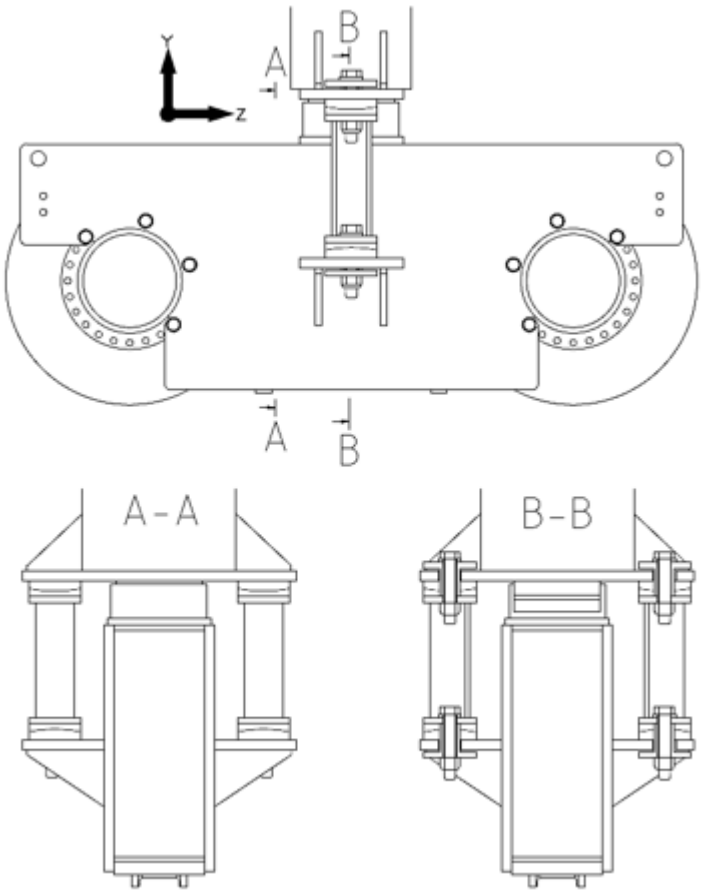

Figure 29. Variant 2.

In the situation of great F_x, it is possible to collapse the bogie if there is no uplift restriction in pot bearing itself or somewhere in the surrounding structure on opposite side of compression profile. In the equilibrium state, when proportions of r_1 and r_2 are equivalent to F_y and F_x, tilting point can be assumed to be in the upper spherical joint of compression profile. In this equilibrium state, vertical force subjected to pot bearing is zero and force F_{screw} subjected to opposite side screw is also zero. Compression in U-profile or N_y is equivalent to vertical rail wheel force F_y. If F_x is increased from this equilibrium state, F_{screw} starts to act preventing rotation and same time increasing N_y if F_y remains constant. Force diagram for variant 2 lower joint is presented in figure 30 according to the described situation where compression in pot bearing is not acting anymore. Horizontal force transmitting capacity of pot bearing was considered full scale even in vertical force was zero. This is due to the reason that horizontal displacement of the bearing piston is constrained by the pot sidewalls.

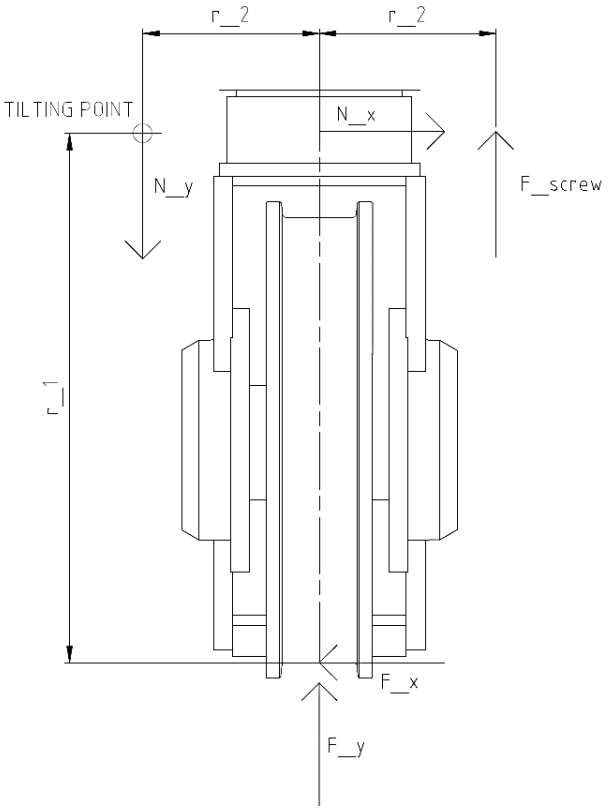

Figure 30. Force diagram of lower joint for solution variant 2.

Things that were checked for variant 2 to ensure preliminary competence of the structures were the following:

- Axial capacity of the screws

- Buckling capacity of the U-profile
- Fatigue loading capacity of the welded joints of U-profile structure.

All the calculation steps for variant 2 were based on same equations (1-7) than calculations of variant 1. Subscripts ($_t$ or $_{tube}$) were replaced by ($_u$) indicating the U-profile. Calculation process for axial, buckling and fatigue calculations is the same with two exceptions. Moment of inertia of the U-profile I_u needed to be calculated in a bending plane leading to smallest value for the measure in question because with round tube, due to symmetry moment of inertia is constant and not dependent on bending direction. Other difference was the determination of imperfection parameter α_u. For U-profile, parameter α_u in the same yield strength class is 0.49 (SFS-EN 13001-3-1 2018, p. 56-57). Buckling calculation carried out in presented way covers competence proofing of the U-profile for flexural buckling of a column. More complex buckling form of a column or buckling of the plate fields of U-profile were considered to include in detailed design. Rest of the parameters for variant 2, modified equations and calculation process is presented in appendix II.

3.4.3 Variant 3 & 4

Variants 3 and 4 were both based on the fork support principle. Variant 4 is more sophisticated and developed version compared to variant 3 which is a straight forward application of fork support principle. Fundamental difference in variants 3 and 4 compared to variants 1 and 2 is the direction of forces, preventing bogie collapsing. In variants 3 and 4 supporting force of a fork support F_{fork} is horizontal, acting against F_x with moment arm r_3. Because F_{fork} is horizontal, all vertical force is subjected to travel straight through pot bearing if friction between F_{fork} providing structural member and side of the bogie is assumed to be zero. Force diagram for variants 3 and 4 is presented in figure 31.

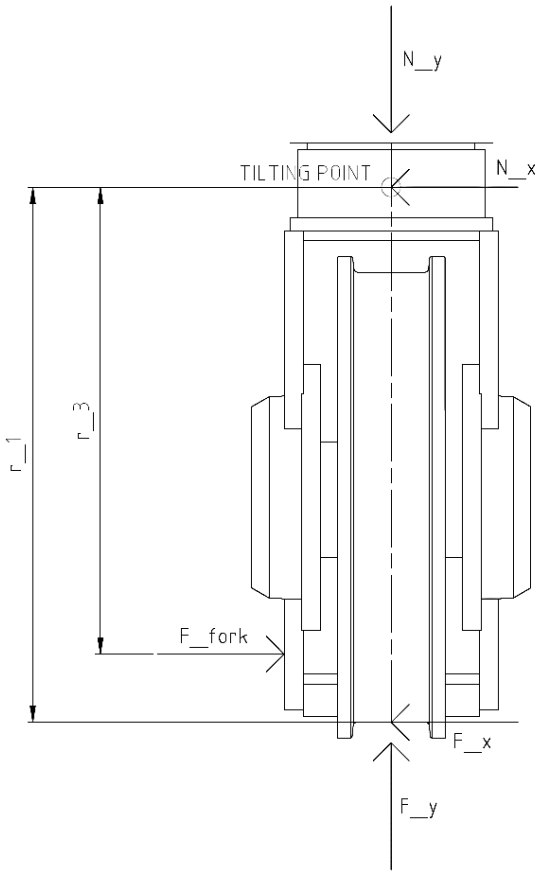

Figure 31. Force diagram of lower joint for solution variants 3 and 4.

Variant 3 utilizes the fork support principle straight forward. Fork plates on both sides of bogie prevent collapsing of bogie with horizontal force F_{fork} which acts between sliding member and bogie frame side plate. High strength polymer or soft metallic sliding member is narrow thus allowing y-rotation according to the fork support principle. Rotation around x-axis is allowed by sliding of the sliding member in relation to bogie frame side wall with a swinging kind of motion, again rotation axis being in the centrum of pot bearing. F_{fork} causes bending moment and shear force to the fork plates. Maximum bending moment M_{max} for the fork plate is in the point where plates are connected to the balancing beam leg structure and shear force is constant over the whole length of independent fork plate. Maximum horizontal force F_x being so great, bending resistance W of one fork member must be respectively great. Aspects regarding x-rotation and bending resistance of fork plates are also applicable in this way for variant 4. Variant 3 is presented in figure 32.

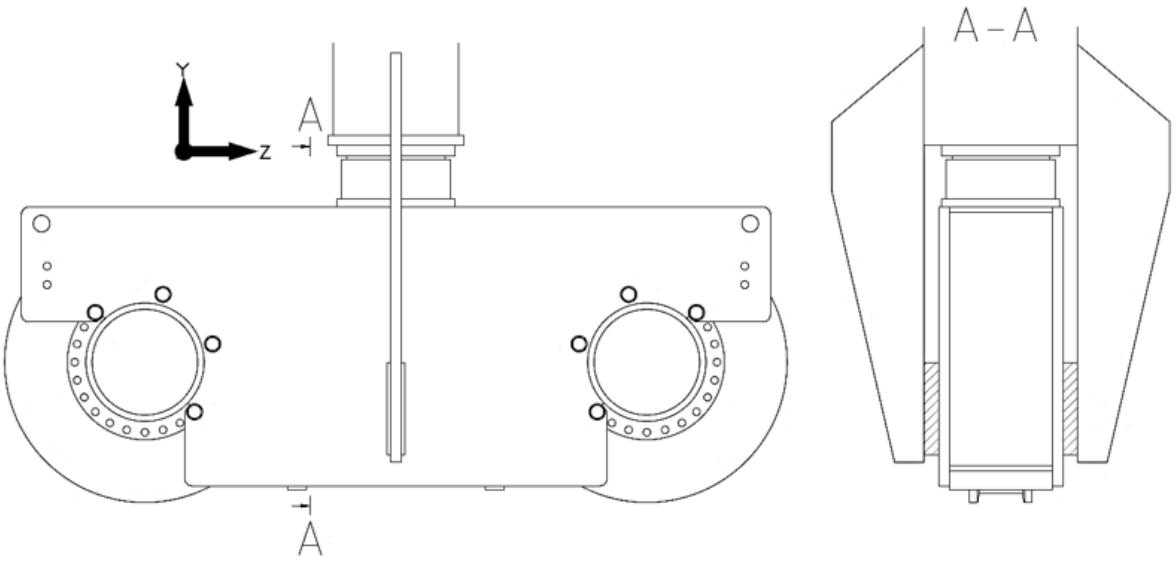

Figure 32. Variant 3.

Basic idea in variant 4 is the same than in variant 3 but configuration of sliding members enables more sophisticated contact between sliding members and bogie frame side wall during y-rotation. Variant 4 presented in figure 33 utilizes spherical caps like in variants 1 and 2 but in different directions and locations. The sliding members are dealt in to two spherical caps per side, having a surface radius matching to virtual spherical surface radius which center point is located on same vertical axis than the rotation center of the pot bearing. This enables the inner convex spherical caps to rotate around the center point of the virtual spherical surface while sliding against the concave spherical caps. Sliding members can be placed through the fork structure and then be secured with bolt connected base plate. Wearing of the sliding members can be compensated by placing thin shim plates between concave spherical cap and base plate.

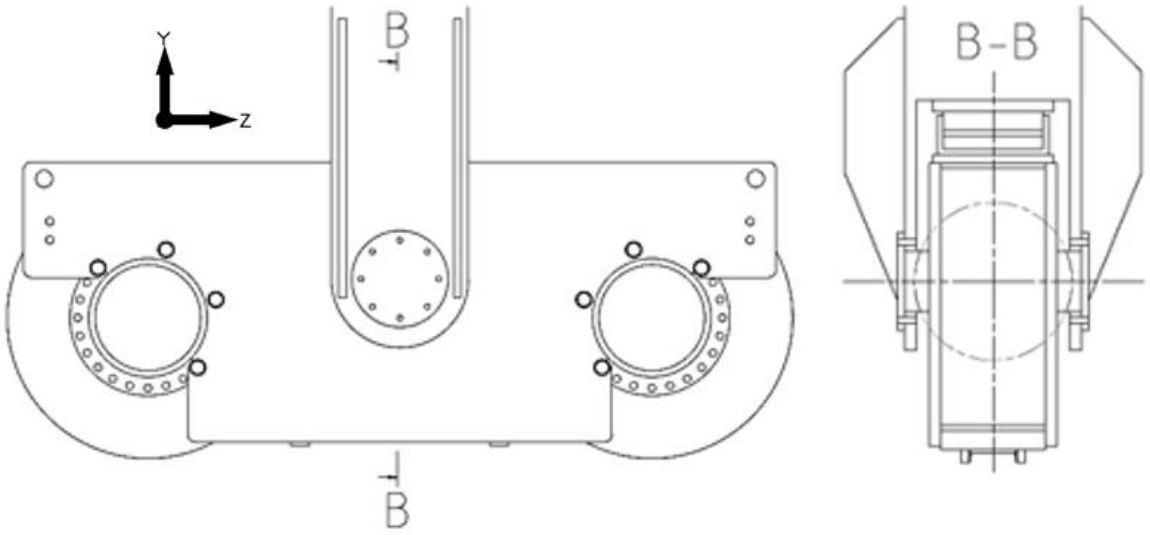

Figure 33. Variant 4.

Things that were checked in preliminary stage for variants 3 and 4:

- Moment capacity of fork structure
- Shear force capacity of fork structure
- Fatigue capacity of fork structure.

For calculating required *W* for fork structure in the maximum static force case, the following equation was utilized:

$$W = \frac{\gamma_m F_{fork} r_3}{\sigma_{y\_fork}} \tag{8}$$

In equation 8, σ_{y_fork} is the yield strength of fork structure material. Ensuring shear force capacity of effective cross-section area of fork A_{fork} (in the lower end of the fork structure where loading causes almost pure shear stress) was calculated with the following equation:

$$\tau = \frac{\gamma_m F_{fork}}{A_{fork}} \tag{9}$$

In equation 9, τ is shear stress in the cross-section. Preliminary calculations for adequate cross-section area against shear force was checked just for certainty because in structures under bending moment will have enough cross-section area to fulfil also shear force requirements but, in this case, where force is great and moment arm relatively short, the effect of

shear force in structure under bending loading is relatively much more significant than in longer bending members.

For fatigue calculations service life cycles for fork structure N_{fork} was ensured in a way that range of normal stress due to bending would be equal or lower than limit design stress range $\Delta\sigma_{Rd}$ when fatigue loading was subjected to a bending beam with bending resistance W. Equation 7 was utilized in fatigue calculations also for fork structure. All calculations regarding variants 3 and 4 are presented in appendix II.

As a principle, turning the fork upside down, the structure would work practically in the same way. Fork pointing upwards, spatial problems could be much more easily handled because traversing machineries wouldn't be on way. Problem is with that kind of configuration that direction of F_{fork} turns to opposite, increasing N_x significantly, making pot bearing and its fixation structures and components much more vulnerable. Clarification of the upside-down fork configuration and its fundamental problem is presented in appendix II.

3.5 Evaluation & selection of best solution variant

For selection of the best option(s) from presented solution variants 1-4, evaluation of variants was carried out. Evaluation process was based on the principles presented by Gerhard Pahl and his co-writers. Process presented by Pahl has references to VDI (Verein Deutscher Ingenieure – association of German engineers) guideline 2225. Process carried out in this study had three main steps: Criteria determination, value assessment and selection. (Pahl et al. 2007, p. 192-197.) Goal of the evaluation was to give answer for overall best solution in numerical form. Results of the preliminary calculations showed that fatigue is not a problem in any of the presented variants and dimensional requirements for the components are in reasonable scale, making all the variants possible in terms of size of individual components.

First step of the evaluation process was to determine criteria, both technical and economic, for the evaluation. Criteria was derived from requirements list with the exception that interfering with machinery components was deleted because it was acknowledged that transmission and motor configuration can be easily modified by changing the stance of the configuration, making more space for the supporting structures. For retrofit installation, stance can

be also changed with certain challenges, but original stance and spatial issues weren't considered as a problem because the transmission and motor configuration is easy to change in cranes yet to be manufactured. (Pahl et al. 2007, p. 194.)

Parts of the technical criteria were the following:

- Simple operation
- Few components
- Low y-rotation resistance
- Detaching with z-movement.

Criterion of simple operation describes how the supporting structures handle the required DOFs and how clear it is to determine which spots are the interface in sliding and rotation. Criterion of few components is self-evident, describing the simplicity of the structure by number of components. Criterion of low y-rotation resistance is an addition for simple operation describing not the operation itself, but sensitivity of the joint for y-rotation. Criterion of detaching bogie with just Z-directional movement is a binary describing the ease of maintenance if it is necessary to detach a bogie from balancing beam for example for wheel of bearing change.

Economic criteria were based on the terminal operator's point of view. Material and production costs of simple and compact components doesn't play that big role compared to the costs caused by maintenance and usage breaks of the crane. Economic criterion was dealt to following three parts, all related to possibly wasted operation time and maintenance costs:

- Simple wearing parts
- Ease of assembly
- Quick maintenance.

All the criteria were weighted equally because lack of specific information concerning details of the variants. Because of vague properties of the variants, numerically presented values for evaluation were built up based on qualitative impression on the variants. In practice this means that variants were compared to each other in every part of criteria and valued with

scale of 0-4 according to VDI principles. (Pahl et al. 2007, p. 194-195.) Evaluation of solution variants is presented in table 10. Solution variant 3 was evaluated the best from the presented alternatives.

Table 10. Evaluation of solution variants (mod. Pahl et al. 2007, p. 195-196.)

Criteria \ Variant		**V_1**	**V_2**	**V_3**	**V_4**
T	Simple operation	1	1	4	3
e	Few components	0	1	4	3
c	Low y-rotation resistance	3	3	4	4
h	Detaching with z-movement	4	4	0	0
Total =		8	9	12	10
Percentage technical =		**0.50**	**0.56**	**0.75**	**0.63**
E	Simple wearing parts	3	3	4	3
c	Ease of assembly	1	2	3	3
o	Quick maintenance	2	2	3	4
Total =		6	7	10	10
Percentage economical =		**0.50**	**0.58**	**0.83**	**0.83**

4 EMBODIMENT DESIGN

In the phase of embodiment design, the joint is given its final layout form based on selected concept solution variant. Results of embodiment design should present the final form of a product and all necessary information for production should be ready. In this study, calculations proofing adequate dimensions for structures and components are presented in own separate chapter “5 Structural analysis”. Shapes, materials and arrangement of the structure and components are designed and selected in the phase of embodiment design and final dimensions are proofed based on preliminary layout for structural analysis. (Pahl et al. 2007, p. 227-229.)

4.1 Layout alternatives

Starting point for layout design was that how the fork plates and pot bearing according to solution variant 3 could be joined to the existing structure presented in figure 35. Problem in joining existing balancing beam leg and fork plates to each other is that fork plates must be positioned in middle of the bogie, meaning that they will be also middle of the side of the balancing beam legs. As shown in figure 34, the existing leg has two inclined web plates symmetrically inside. If fork plate is connected to middle of the flange plate, there is no stiff member behind the flange plate, subjecting it to high stresses.

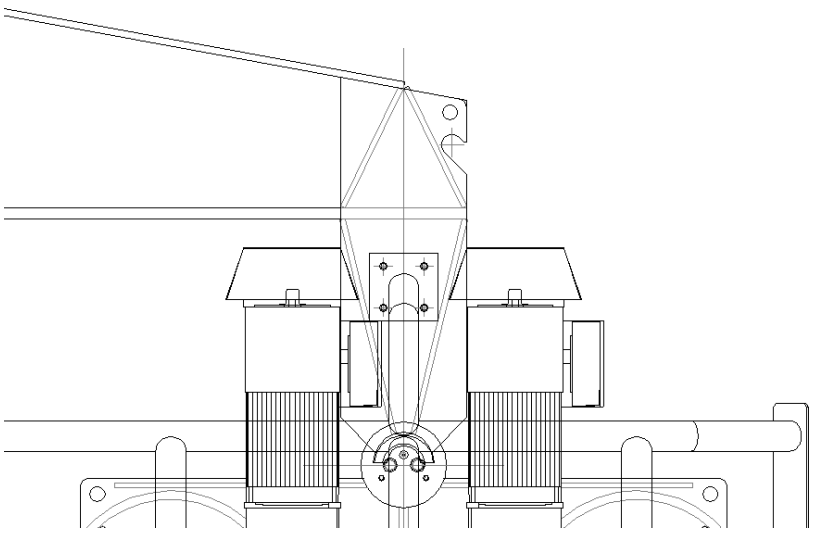

Figure 34. End of balancing beam, balancing beam leg and lower joint (Konecranes 2018c).

Because of the positioning of the web plates of balancing beam leg, interface for existing structure and retrofit structure must be moved upwards, making it possible to construct stiff enough fixing point for the fork plates. Requirement for stiff middle area of flange plate led to idea of one web plate, in middle of the leg profile. In practice this meant I- or H-profile resembling balancing beam leg profile. Other option would have been a structure with two original web plates and a one additional web plate between them, but this kind of plate structure configuration was considered too complex in means of welding assembly. Weld inspection in the inner plates of the structure would have been also much more difficult so the three-webbed design was neglected already in the starting point of layout design. Totally new balancing beam leg also enables smoother stress flow because constraints proposed by the configuration of original balancing beam leg could be avoided. Connection of I- or H-profile to the end of balancing beam is simple. Draft for base layout of the balancing beam leg including pot bearing fixing plate is presented in figure 35. Flange plates of the profile are subjected to travel almost to the bottom level of bogie frame. Flanges of balancing beam leg are also utilized in the actual fork structure. Draft presented in figure 35 is drawn without the actual bending resistance providing fork plates and leg interface for balancing beam end is simplified as a horizontal plane. Top plates of the bogie frame are arranged in a way that top of the bogie is flat, providing fixing base for pot bearing lower part.

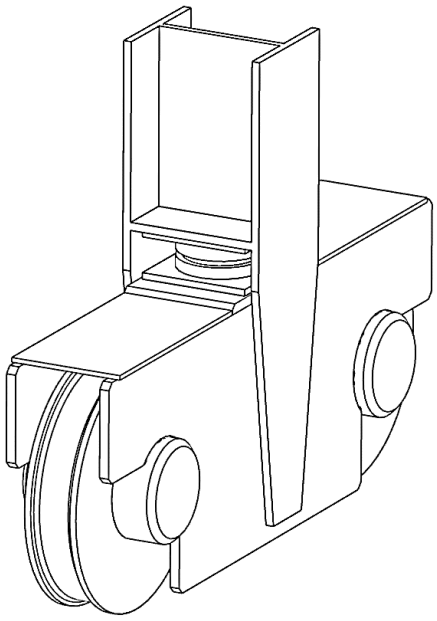

Figure 35. Draft of base layout.

Arrangement of structures and components are constructed according to draft of base layout. Material for the structures is scoped to EN 10025-2 compatible S355 structural steel or its equivalent according to other standards. High strength steel could be a good option because according to load definition, static loading is critical, not fatigue loading, so capacity of high strength steel could be fully utilized if increased deflection due to lower bending resistance doesn't cause additional problems. Weight of the structure would be lower but due to challenges of welding high strength steel and possible differences between simplified and actual fatigue loading, S355 or equivalent was selected.

Arrangement of structures and material being selected, shape of the bending resistance providing fork plates was the next thing to be defined. Critical point for fork plates is the point where pot bearing is fixed, and fork plate connected to the web plate of balancing beam leg. This is the point where maximum bending resistance is required for the fork plates. Two different cross-section profiles were considered for the fork structure. T- and asymmetrical H-section. Drafts of sections are presented in figure 36. T-profile is simpler, but it requires greater height to achieve similar bending resistance than H-section and due to wider plate sections with free edges, it is fundamentally less stable than H-section. Asymmetricity of H-sections is not desired property, but it is required to ease assembly and disassembly of wearing parts setup on the lower ends of the forks.

Figure 36. Options for fork structure cross-section.

Bending resistance for both optional cross-sections was calculated, and results compared to the required bending resistance calculated in appendix II, page 5. Bending resistance was calculated with the following equation:

$$W = \frac{I_{fork}}{c} \tag{10}$$

In equation 10, I_{fork} is the moment on inertia of cross-section in question and c is the distance from neutral axis to edge of cross-section normal to neutral axis. For determination of I_{fork} and c for both cross-sections Siemens FEMAP 11.4.2 FEA modelling software was utilized. Defining of cross-sections and bending resistance calculations are presented in appendix III. H-section with the main dimensions presented in appendix III was selected for fork structure because of great height requirement for web plate of T-profile.

4.2 Preliminary layout for structural analysis

By adding the bending resistance providing members to the base layout, preliminary layout for structural analysis was created. Ends of the T-profile's webs and flanges were chamfered in the end areas. Because of width of the balancing beam end, top part of the leg had to be narrowed and because of greater width of bogie frame, flanges of the leg had to be inclined to provide enough space for bogie frame. Flange plates themselves were kept straight to enable simpler manufacturing without additional horizontal stiffeners and to enable smoother stress flow. Compensation for the inclination of flange plates was carried out in the wearing part geometry. Simplest form of wearing parts is a plate welded on its edge and this kind of configuration was used in the structural analysis. More sophisticated and detailed wearing parts configuration was considered as a future study aspect. It must be noted that bogie frame used in the 3D-models is for rail wheel size 710 mm meaning that the contact point between bogie frame and wearing part is much lower than in the figures. Preliminary layout for structural analysis and further detail development is presented in figure 37.

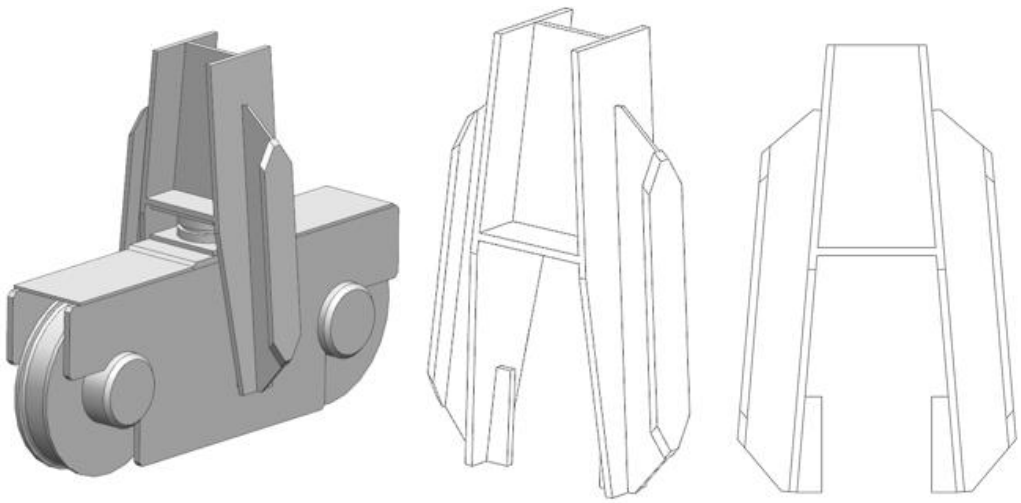

Figure 37. Preliminary layout for structural analysis.

5 STRUCTURAL ANALYSIS

Structural analysis was carried out for the support structure including the leg and the forks and for the fixing components of the pot bearing. Interface for connection of leg and balancing beam end was placed in the horizontal plane between them, as described earlier in draft of base layout in figure 35. Bogie frame and balancing beam were scoped out from the analysis. Criterion for structural competence was maximum static capacity, still staying on the elastic zone. FEA was utilized with support structure and fixing components were analyzed based on analytical calculations based on standard SFS-EN 13001-3-1. Loading data for both analyses derived from preliminary calculations of solution variants 3 and 4 is presented in table 11.

Table 11. Loading data for structural analysis.

r_1	740	[mm]
r_3	590	[mm]
F_x	384	[kN]
F_y	932	[kN]
$\Sigma M=0$		
$F_x r_1 - F_{fork} r_3 = 0$		
F_{fork}	**481.6**	[kN]
$\Sigma F=0$	Horizontal	
$F_x - F_{fork} + N_x = 0$		
N_x	**97.6**	[kN]
$\Sigma F=0$	Vertical	
$F_y - N_y = 0$		
N_y	**932**	[kN]

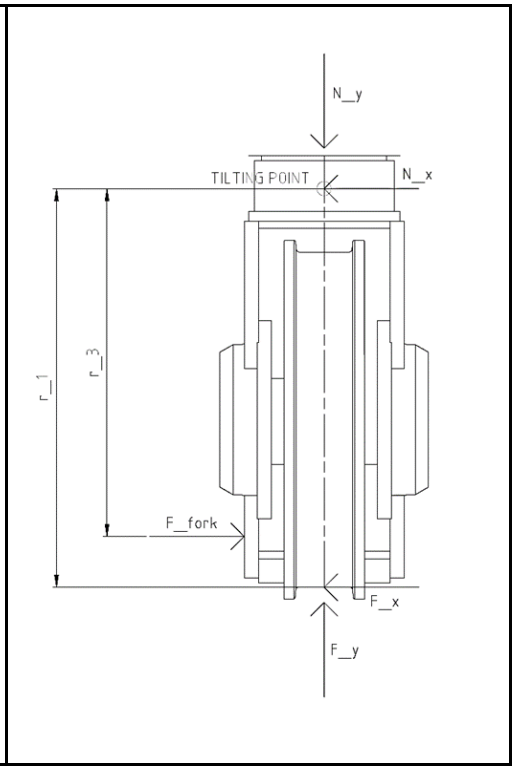

5.1 Support structure

FEA for support structure was carried out with Siemens FEMAP 11.4.2 pre- and postprocessing software which utilizes NX Nastran solver in the calculation stage. First step of the analysis was to create geometry for the structure. Geometry was created by drawing middle

surfaces of the plates of the structure. Symmetricity of the structure was utilized, and only other half of the support structure was drawn. Because plate thicknesses affect the positioning of the middle surfaces, 25 mm plate thickness for all plates was selected for a starting point which then could be modified according to results of the first rounds of static analysis.

Half of the support structure was meshed with 15 mm 4 noded quad and 3 noded tri -plate elements with automatic mesh surface tool. Then the elements were copied and rotated to the opposite side. As mentioned before, interface between leg and balancing beam end is the horizontal plane in the top end of leg. Plate edges connecting to this surface were fixed rigid on every node on the plate edges. Meshed plate structure and placing of fixed constraints can be seen in figure 38. Material properties given for the elements was elastic modulus E 210 GPa and Poisson's ratio 0.3. Own weight of the support structure was not taken into consideration.

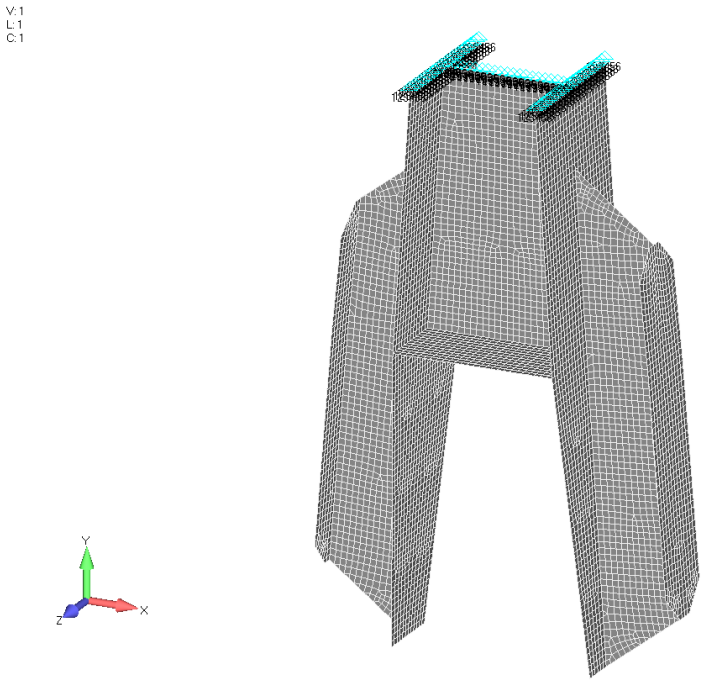

Figure 38. Meshed plate model and fixed constraints.

Loading was set on nodes at the connection point of wearing parts and under the web plate of leg. Total forces were distributed equally on all nodes under the influencing area of the load in question. Assumption was made that all vertical force from pot bearing is subjected to the web plate of the leg. N_x was also subjected to the web plate of leg because in the

situation where vertical force is great, friction between pot bearing top and fixation plate is enough to transmit the horizontal force and screws would be just a safety measure. Structural competence of screws is proofed later but for the purposes of structural analysis of support structure, these mentioned assumptions were used. Figure 39 presents loading on the structure. Loads under fixation plate includes both x- and y-components for N_x and N_y.

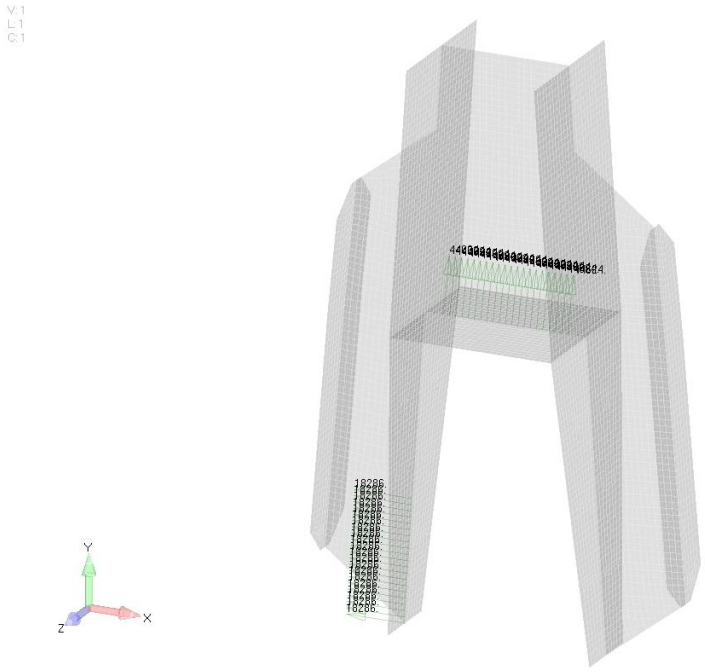

Figure 39. Loads for the supporting structure.

After meshing of the geometry and setting of loading and constraints, linear static analysis was carried out. Limit design stress *lim σ* was calculated with the following equation (mod. SFS-EN 13001-1 2015, p. 44):

$$\lim \sigma = \frac{\sigma_{y\_fork}}{\gamma_m} \tag{11}$$

With the preliminary configuration of 25 mm plate thickness of every plate, competence of the structure appeared to be sufficient except in the top part of H-profile and especially the connection point of fixing plate and leg flange. Results of the analysis are presented as Von Mises stress for the preliminary layout in figure 40. Calculation for *lim σ* is also presented in the same figure. Dashed ellipses present the areas where Von Mises stress is over the

allowable value. Stress peaks in the sharps corners can be ignored but in both marked areas, high stress is not only in the very corners but also spread with distance of several elements. Due to material linearity of the analysis, stresses above yield strength don't act according to practice. In practice stress in the areas where yield strength is exceeded would spread wider due to plasticity and actual stress state would be lower than what the figures present.

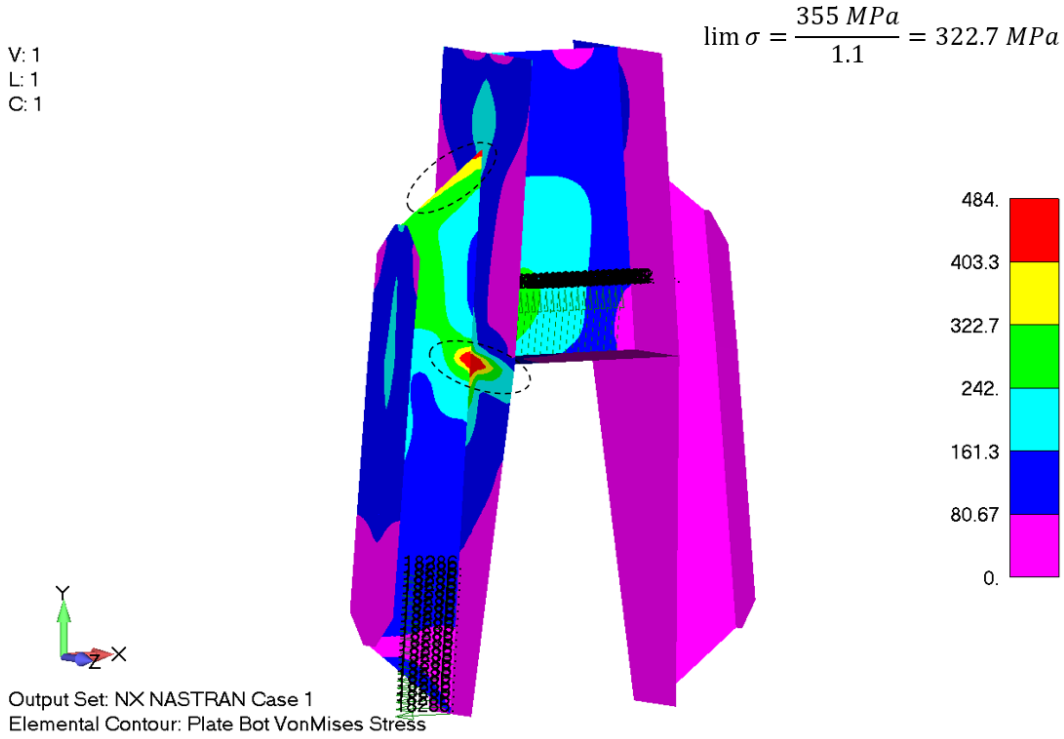

Figure 40. Von Mises stress for preliminary layout.

Structure would have been probably sufficient as it is but the size of the area of yield strength exceeding stress state was considered too great to avoid problems of possible local plasticity. Means for decreasing stress state in the marked areas without increasing plate thicknesses was to stretch the outer flange of H-profile to continue over the curve and then connect it to the flange of leg and adding horizontal stiffener inside the leg profile. Other option was to position the outer flanges vertically, providing more bending resistance in the critical area of pot bearing fixing plate and moving the H-profile web plate connection upwards. Fundamentally the first option would be better because it would close the free edge of H-profile web but due to simpler manufacturing the second option was selected to further analysis. Schematics of both options are presented in figure 41.

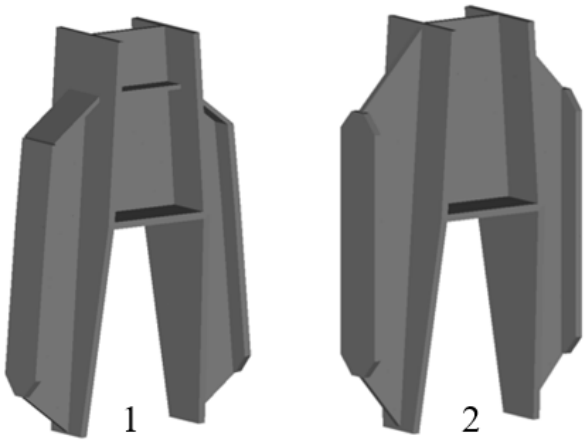

Figure 41. Schematics of optional structures.

FEA-model was created for the second option of further development of preliminary layout with the same exact steps and definitions than for the original preliminary layout. Parameters for meshing, constraints and loading were the same, just the extension of the H-profiles were conducted. Results of static linear analysis for preliminary layout's second development option is presented in figure 42. Areas of stress concentration are marked with dashed ellipses.

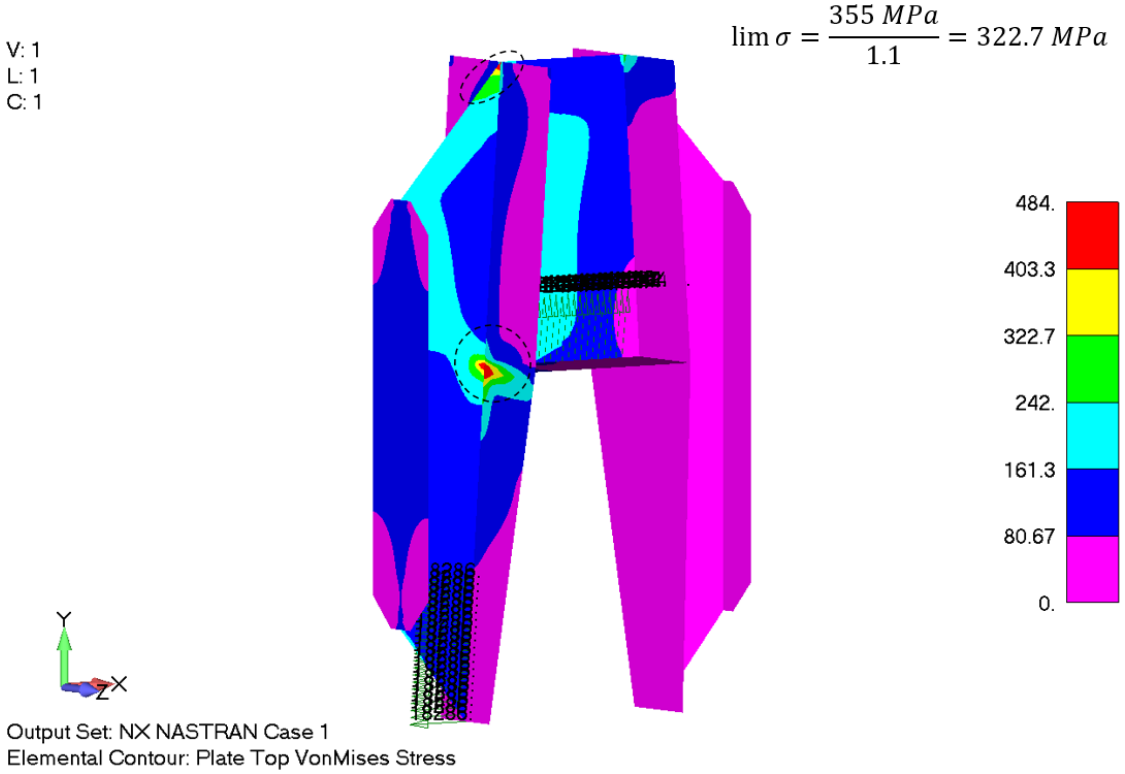

Figure 42. Von Mises stress for second development option of preliminary layout.

In second development option, extending the web plate of H-profile decreases Von Mises stress in the top end area of the plate in question. Widening the web plate by positioning the outer flange vertical decreases the area of stress peak in the connection point of pot bearing fixation plate and leg flange. With these minor changes to preliminary layout, static strength of the layout was proofed to be adequate. Stability of the structure was checked by running linear buckling analysis for the structure. Plate thicknesses being so great compared to widths of each separate plate section, plate buckling wasn't expected to happen. For the result of buckling analysis, first eigenvalue was obtained which defines how many times the applied loading must be multiplied to cause first buckling form. Linear buckling analysis doesn't take geometrical imperfections into consideration and therefore the eigenvalue equivalent multiple is a multiple for ideal structure. As anticipated, first buckling form wasn't plate buckling but lateral-torsional buckling of the H-profile. Buckling form and eigenvalue is presented in figure 43.

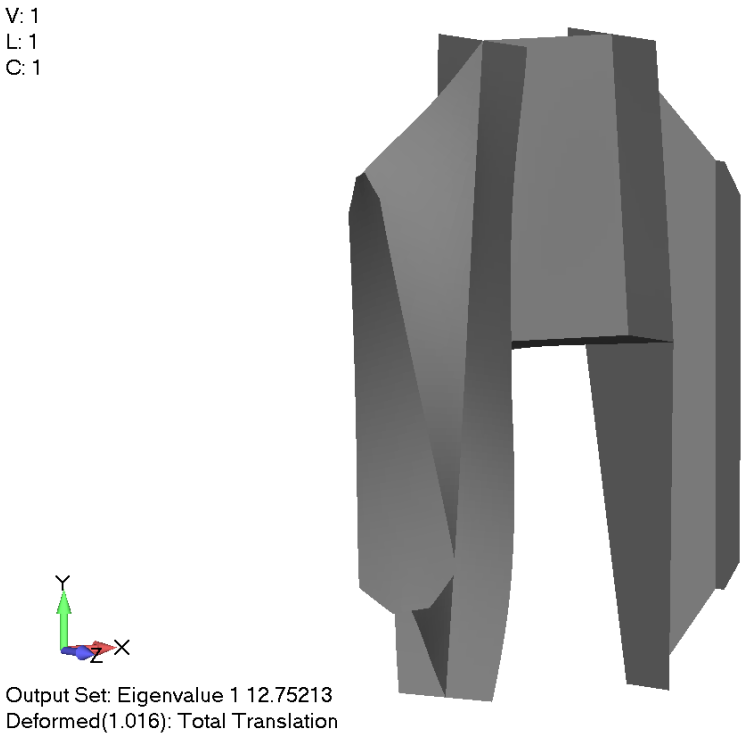

Figure 43. Lateral-torsional buckling of H-profile of support structure.

With eigenvalue of 12.75 it can be said that even with geometric imperfections of the structure, loading causing stability loss for the structure is impossible to gain in the bogie assembly. If loading in some case exceeds the values used in the calculation, other components or

structures will yield before stability loss happens and even in this case, the support structure has yielded earlier before buckling. If plate sections used would be thinner, buckling problems could occur and they should be threaded with required stiffening manors.

5.2 Fixing components

Pot bearing is fixed to its fixing plates with four screws on both top and bottom part. Because vertical force travels straight through the bearing, in normal use the screws are subjected only to shear loading in one plane. Vertical force is assumed to be always great enough to keep the pot and piston of the bearing on contact with the fixing plates and therefore eliminating the possibility for bearing tilting and normal force for the screws. Holes in the fixing plates may be threaded or optionally a nut would be on the opposite side, but this doesn't affect the shear capacity of the screws. If the bearing is equipped with anti-uplift device inside the bearing, then the screws must be able also to withstand normal force due to weight of bogie including machineries and other accessories in the case of possible uplift. If anti-uplift devices are placed outside the bearing, then the screws will not be subjected to normal force due to external loading. Tightening of the screws will induce normal force for the screws, but because intention is not to create friction grip connection, normal force due to tightening was considered low and therefore neglected from the calculations. Friction grip connection would be better than shear connection for the type of joint, but the low number of fixing holes of pot bearings prevent the possibility for greater amount of screws and thereby the possibility for friction grip connection. Fixing holes of pot bearing and type of loading is presented in figure 44.

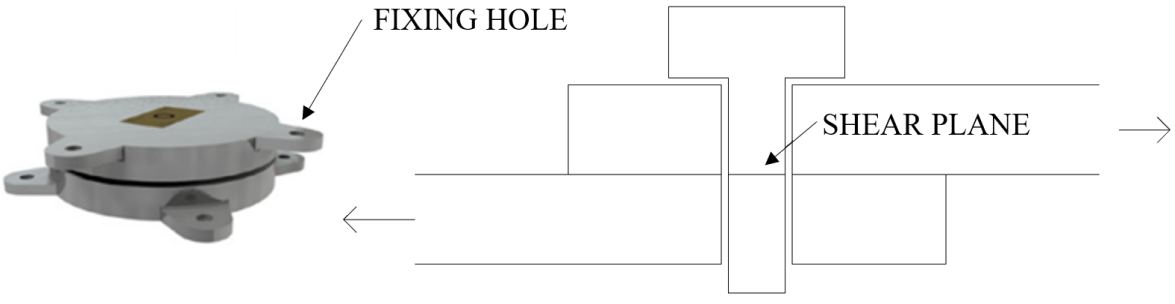

Figure 44. Fixing holes of pot bearing and type of loading.

To proof the competence of the pot bearing fixing, limit design shear force $F_{v,Rd}$ for the screw and limit design bearing force $F_{b,Rd}$ for fixing plate and screw connection were calculated. $F_{v,Rd}$ was calculated with following equation (mod. SFS-EN 13001-3-1 2012, p.23):

$$F_{v,Rd} = \frac{f_{y\_screw} A_{screw}}{\gamma_m \gamma_{sbs} \sqrt{3}} \quad (12)$$

In equation 12, γ_{sbs} is specific resistance factor for bolted connections and its value is dependent on the fact that is there multiple or just one shear plane in the connection. For single shear plane connection γ_{sbs} is 1.3. (SFS-EN 13001-3-1 2012, p. 23-24.) $F_{b,Rd}$ was calculated with following equation (mod. SFS-EN 13001-3-1 2012, p.24):

$$F_{b,Rd} = \frac{\sigma_{y\_fork} dt}{\gamma_m \gamma_{sbb}} \quad (13)$$

In equation 13, d is the shank diameter of screw, t is the thickness of pot bearing fixing plate and other plates of the structure and γ_{sbb} is the specific resistance factor for bolt connections and it is also dependent on the number or shear planes. For single shear plane connection γ_{sbb} is 0.9. Yield strength of fixing plate material was selected for the equation because it is lower than respective value of the screw material. (SFS-EN 13001-3-1 2012, p.24.) Requirements for using equation 13 are the following (SFS-EN 13001-3-1 2012, p.24):

- Distance from hole center point to edge of plate must be 1.5 times the hole diameter
- Distance between holes must be 3.0 times the hole diameter.

These requirements were fulfilled with the dimensions of the fixation plate and fixing screws. Fundamentally shear connections or shear force being the dimensioning measure should be avoided and the connection itself shouldn't be on the area of threads due to smaller cross-section area and sharp geometry changes (Kemppi 1992, p. 154). Because of low number of fixing holes in the pot bearings, shear connection cannot be avoided but using enough long screws and possible spacers between nut and plate, shear plane can be easily moved to the shank of the screws not dependent on the dimensions of the screw. Due to slipping and displacements in the joint, in elastic state, shear force was assumed to act only on two screws. If bearing capacity of the fixing plate is smaller than shear capacity of screws, plasticity in the hole areas would eventually even the shear forces for all four screws. But because in this state the holes would be elliptical and minor failure could be considered, stresses were limited to act only on elastic region and thereby for only two screws. (Kemppi 1992, p. 154-158.) Screw size M16 and strength class 8.8 were used as preliminary values for connection. Calculation for connection is presented in appendix IV and result compared to N_x.

6 DEFINITIVE LAYOUT

Definitive layout for the pot bearing supporting fork structure is the result of this study. According to the systematic product development process, definitive layout is the final version of the product in question before producing manufacturing documentation based on the layout (Pahl et al. 2007, p. 227). Detailed documentation is not presented in this study but clear presentation of the definitive layout for the steel structure and fixing of pot bearing is shown in figure 45. Required modifications for the bogie frame are also presented in the figure even if more detailed design of bogie frame was scoped out from the study.

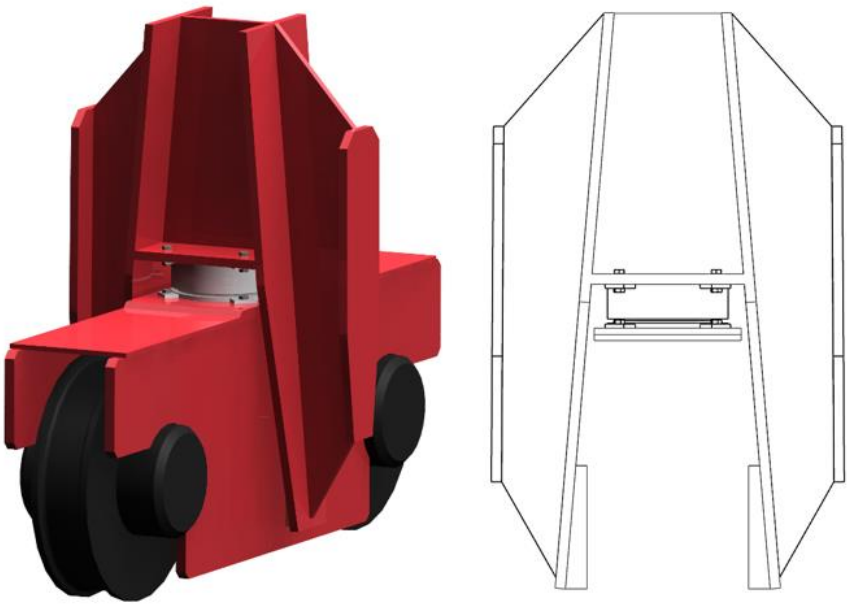

Figure 45. Definitive layout of pot bearing lower joint and supporting structure.

Main properties of the fork supporting structure are presented in table 12. Dimensions for plate thickness and screw sizes are minimum requirements.

Table 12. Main properties of definitive layout of pot bearing supporting structure.

Max F_x	384	[kN]
Weight	387	[kg]
t	25	[mm]
Fixing	M16 8.8	(8 pcs)

7 DISCUSSION

New engineering solution for lower joint of RMG bogie assembly was found as a result of this study. New joint solution can be retrofitted to the crane studied with certain challenges and to new cranes with modified bogie assemblies. Calculation methods used in the loading study are usable for different size of gantry cranes and amount of enforced skewing but needs to be confirmed with measurements to obtain adequate safety or to get rid of excessive safety enabling lighter structures. New lower joint design can be utilized also in other kind of joints in wider application area than just cranes. If some structure requires the same degrees of freedom and some loading directional elasticity in the joint, layout of the lower joint can be modified to suit the requirements of the structure in question. Functionality and structural competence of the lower joint assembly must be proofed before implementing the joint to bogie assemblies of cranes offered to customers.

7.1 Interface with existing structure and designed lower joint

In cranes yet to be manufactured, spatial problems don't occur because selection of measurements of balancing beams, bogies and machinery configuration is practically free compared to a retrofit situation. In a retrofit situation the connections of balancing beam and top section of the fork structure can be handled quite easily but traversing machineries in the bogies induces spatial constraint for the structure. This can be avoided by changing the transmissions to an upright version of the same transmissions and utilizing the existing motors. Traversing machinery configuration modification can be seen in figure 46.

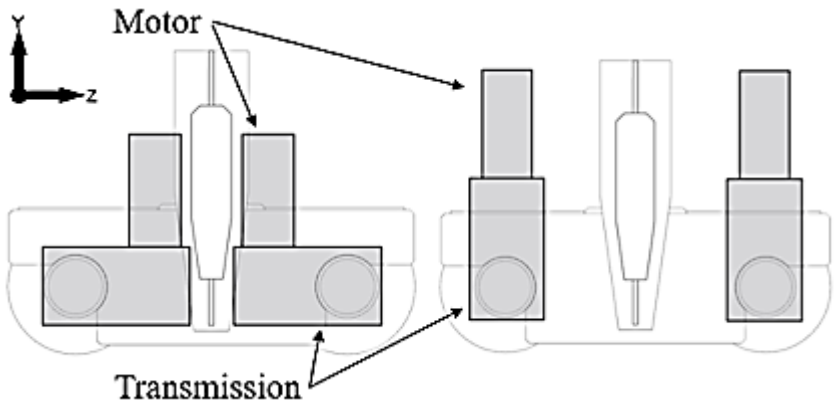

Figure 46. Traversing machinery stance modification.

7.2 Error analysis

Defining of loading both in static and fatigue cases was simplified in the means of constraints and loading cases. Enforced skewing and horizontal forces caused by it where considered just a contact force between flanges of outermost wheels and rail sides. Friction between other wheels and rail top was neglected. This simplification causes most probably higher horizontal forces to the outermost wheel pairs compared to the situation that friction would have been included in to the calculations of enforced skewing loading case. Model for rail deviation induced fatigue loading was also highly simplified because of lack of information of the actual rail deviations in the terminal of the studied crane. Fatigue loading amplitude due to rail deviations might vary significantly compared to the model used in calculations.

7.3 Conclusions

Definitive layout of pot bearing lower joint allows the desired DOFs and restricts the unwanted ones and is thereby a considerable option for the lower joint of RMG bogie assembly. Definitive layout is simple and not remarkably heavier than the existing balancing beam leg/lower joint assembly. Increased manufacturing costs are acceptable because of better functionality and decreased amount of maintenance which decreases the overall operating costs of the crane and increases attractiveness of the crane. Presented solution can be applied as a factory solution or a retrofit installation.

7.4 Novelty, generalization and utilization of definitive layout

Pot bearings have not been used in bogie joints of Konecranes port cranes before. Presented definitive layout can be modified to fit in different types of rail mounted gantry cranes with different magnitude vertical and horizontal loadings in the lower joints. Pot bearings can be procured in various dimensions for various loadings and due to the simplicity of the bearing, tailor made bearings are also easily available. If size and mass of the fork structure is not a problem, dimensioning of the structure for greater loads is also possible practically without restrictions if the required rotation capacity around vertical axis stays relatively small. Definitive layout can be also applied to other non-crane related structures, where requirements for DOFs are similar. Because the solution is not size dependent, the non-crane related structures can similarly present wide range in size, mass and loading magnitude.

Pot bearing can be replaced by a spherical bearing which has the same DOFs than pot bearing, but no elasticity in the bearing normal direction. Wearing parts can be replaced with spherical caps presented in solution variant 4. With these changes and all combinations of the changes, the similar functionality can be achieved for the joint, meaning that the solution is not totally dependent on pot bearing.

7.5 Future development

To be able to proof structural competence of the fork structure, strain gage measurements must be carried out. Maximum static loading happens in a situation of enforced skewing of the gantry, so this loading case is not measured due to possible damages to the components of the crane, but stress data can be used to determine actual stress variations due to rail deviations and thereby develop the fork structure to withstand greater fatigue loading if necessary. In addition to the strain gage measurements, rotation and angular acceleration measurements of the bogie must be carried out around vertical axis of the pot bearing to study sensitivity of whole joint configuration. Results of rotation and angular acceleration measurements are used to determine is rotation around vertical axis happening and if so, how fast the rotation changes are happening.

Development of different kind of wearing parts and wearing parts assemblies will be carried out to find out most suitable material pair for the connection and make assembly and maintenance easy and fast. Definitive solution presents the simplest functioning form of the connection but some wearing component is added between the steel surfaces to prevent excessive wearing. Corrosion aspects are also focused in the development stage of wearing part assembly. Testing of wearing part assembly will be carried out and results utilized to even further develop the components. Other detailed development aspect is the pot bearing itself. In this stage the expertise of pot bearing manufacturer is utilized to develop the product originally designed for static structures to suit better to the constantly moving machine if any challenges related to greater number of orientation changes are faced.

8 SUMMARY

Objective of this master's thesis was to find pot bearing utilizing engineering solution for RMG lower bogie joint which would allow rotation around vertical axis of the joint and rotation induced by height deviations in travelling tracks. Solution had to withstand static and fatigue loading subjected to the joint while maintaining stability of the crane meaning that the bogie was not allowed to collapse under balancing beam due to horizontal force subjected to the rail wheels.

Before starting design work for the new joint, loading for the joint was obtained. Loading cases were based on F.E.M. 1.001 3nd and SFS-EN 13001-2 standards and worst-case loading for the lower joint was enforced skewing of the gantry. This loading was used as a dimensioning criterion against static loading. Fatigue loading was based on enforced displacements caused by deviations in the travelling track. Magnitude and frequency of the displacements were based on simplified model of rail curvature. Rail curvature model was build according to travelling track tolerance class 2 according to standard ISO 12488-1.

After the loading was obtained, systematic development process for pot bearing supporting structure was started by producing requirement list and then abstracting it to find out the main problem. Three different working principles were found and two of them were utilized when sketching solution variants for the joint. Four different solution variants were created and evaluated against each other with technical and economic criteria. Variant 3 or the fork structure was selected for further development and embodiment design.

In embodiment design shape and preliminary dimensions were obtained for the fork structure with analytical calculations. Base layout of the structure was constructed from H-profile resembling beam and adequate bending resistance for the forks was achieved also by mimicking H-profile. More accurate calculation for the structure was carried out with FEA and required modifications were done. After the calculations for the steel structure, competence of the pot bearing fixing screws was proofed and definitive layout of the pot bearing lower joint was created. Measurements and further development of wearing parts will be carried out before standardizing the joint solution for wider use.

REFERENCES

FEMdata. 2018. [Referred 21.10.2018]. Available: http://personal.inet.fi/yritys/femdata/Tuotteet.htm

F.E.M. 1.001 3nd. 1998. Rules for the design of hoisting appliances. Booklet 2. Classification and loading on structures and mechanisms. Paris: European Handling Federation. 62 p.

Freyssinet. 2016. [Referred 21.8.2018]. Available: http://www.freyssinet.com/freyssinet/wfreyssinet_en.nsf/0/91ADDB0FE8CFA883C1257C6A003372B6/$file/C%20V%204_FREYSSINET%20MECHANICAL%20BEARINGS%20EN_V01.PDF

ISO 12488-1. 2012. Cranes – Tolerances for wheels and travel and traversing tracks –. Part 1: General. 2. edition. Geneva: The International Organization for Standardization. 20 p.

Kemppi, J. (editor) 1992. RIL 167-2 Teräsrakenteet II (Handbook on Steel Structures II). Helsinki: Association of Finnish Civil Engineers RIL.

Konecranes. 2018a. [Referred 25.7.2018]. Available: https://www.konecranes.com/about-konecranes

Konecranes. 2018b. [Referred 25.7.2018]. Available: https://www.konecranes.com/equipment/container-handling-equipment/rail-mounted-gantry-cranes

Konecranes. 2018c. Engineering documentation of the company.

Niemi, E. 2003. Levyrakenteiden suunnittelu. Tekninen tiedotus 2. Helsinki: Teknologiateollisuus ry. 136 p.

Pahl, G., Beitz, W., Feldhusen, J. & Grote, K.H. 2007. Engineering design – A Systematic Approach. London: Springer-Verlag. 617 p.

Parviainen, M. 2018. RMG operointidataa [private email]. Receiver: Ari Partti. Sent 22.10.2018 at 7:47 (GMT +0100).

Rautajärvi, H. 2018. RE: G1699 pukin inu [private email]. Receiver: Ari Partti. Sent 3.10.2018 at 11:06 (GMT +0100).

SFS-EN 1993-1-9. 2005. Eurocode 3: Design of steel structures. Part 1-9: Fatigue. Helsinki: Finnish Standards association. 41 p.

SFS-EN 13001-1. 2015. Cranes. General design. Part 1: General principles and requirements. Helsinki: Finnish Standards Association. 64 p.

SFS-EN 13001-2. 2014. Crane safety. General design. Part 2: Load actions. 5. edition. Helsinki: Finnish Standards Association. 123 p.

SFS-EN 13001-3-1. 2018. Cranes. General design. Part 3-1: Limit states and proof competence of steel structure. Helsinki: Finnish Standards Association. 116 p.

The Kansas City Star. 2015. [Referred 25.7.2018]. Available: https://www.kansascity.com/news/business/article11244203.html

Appendix I

Vertical forces for lower joints.

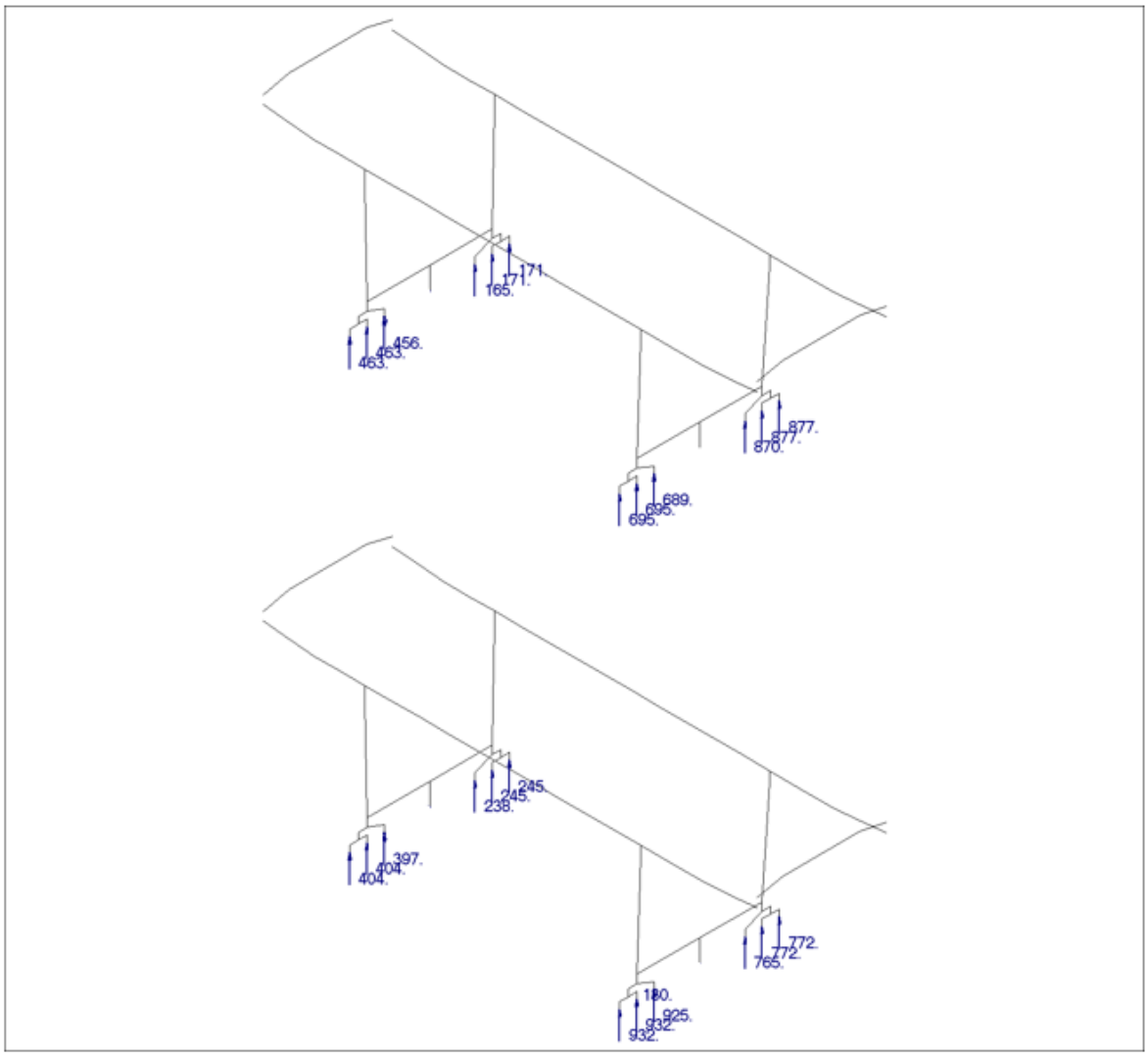

Preliminary calculations for solution variants.

Variant 1

Axial capacity:

r_1	740	mm
r_2	300	mm
F_x	384	kN

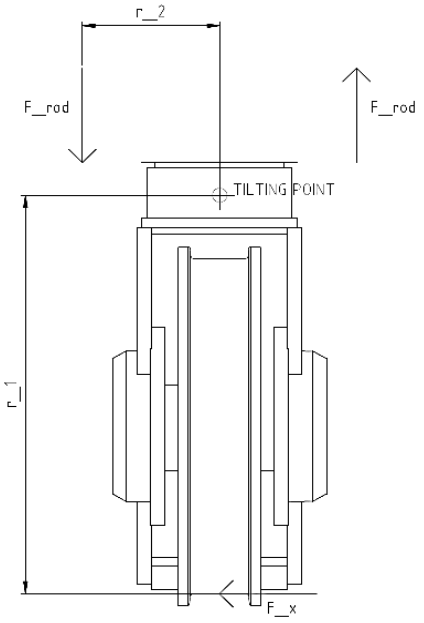

$\Sigma M=0$

$F_x r_1 - 2F_{rod} r_2 = 0$

F_{rod}	**473.6**	kN

$$A_{rod} = \frac{F_{rod}\,\gamma_m}{f_{y\_rod}}$$

γ_m	1.1	

	Tube	Threaded bar 8.8	
f_{y_rod}	355	640	MPa
A_{rod}	**1467**	**814**	mm^2

Buckling capacity:

E	210	[GPa]
D	60	[mm]
d	40	[mm]
I_{tube}	510508	[mm^4]
L_t	500	[mm]

$$N_{k\_t} = \frac{\pi^2 E I_{tube}}{{L_t}^2}$$

N_{k_t}	**4232**	[kN]
f_{y_t}	355	[MPa]
A_t	1571	[mm$^{2]}$]

$$\lambda = \sqrt{\frac{f_{y\_t} A_t}{N_{k\_t}}}$$

λ	**0.3630**

α_t	0.21

$$\xi = 0.5[1 + \alpha_t(\lambda - 0.2) + \lambda^2]$$

ξ	**0.5830**

$$\kappa = \frac{1}{\xi + \sqrt{\xi^2 - \lambda^2}}$$

κ	**0.9623**
γ_m	1.1

$$N_{Rd\_t} = \frac{\kappa f_{y\_t} A_t}{\gamma_m}$$

N_{Rd_t}	**488**	[kN]

Fatigue calculation:

Z	1E+08	[m]
Z_{sample}	160	[m]
N_t	6.25E+05	Re-quired
γ_{mf}	1.05	
ΔF_x	30 000*	[N]

$$N_t = \left(\frac{\Delta\sigma_c}{\gamma_{mf}\,\Delta\sigma_{Rd}}\right)^3 \cdot 2 \cdot 10^6$$

	Tube	Threaded bar 8.8	
$\Delta\sigma_c$	36	63	[MPa]
A_{rod}	1571	814	[mm$^{2]}$]
$\Delta\sigma_{Rd}$	23.55	45.45	[MPa]
N_t	**6.2E+06**	**4.6E+06**	cycles

*Assumption was made that with low amplitude horizontal loading, structure will operate only with one rod structure, not able to utilize both rods.

Variant 2

Axial capacity of screws:

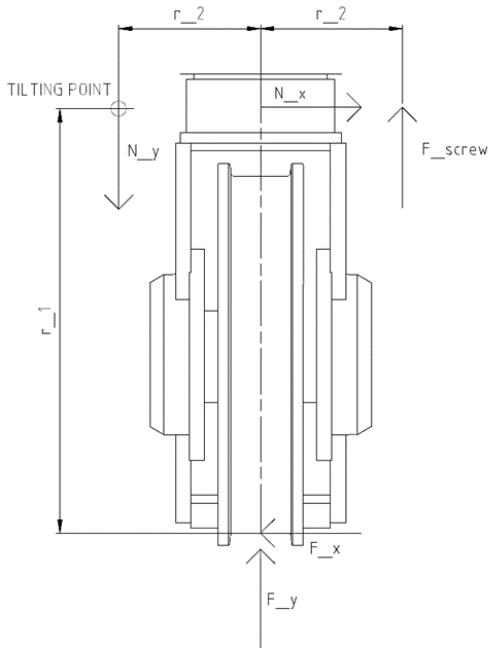

r_1	740	[mm]
r_2	300	[mm]
F_x	384	[kN]

$\Sigma M=0$

$F_x r_1 - F_{screw} 2 r_2 - F_y r_2 = 0$

$\Sigma F=0$

$F_y + F_{screw} - N_y = 0$ Vertical

	Situation 1	Situation 2	
F_{screw}	**0**	**473.6**	kN
F_y	**947.2**	**0**	kN
N_y	**947.2**	**473.6**	kN

F_{screw} **473.6** kN

$$A_{screw} = \frac{F_{screw}\,\gamma_m}{f_{y\_screw}}$$

γ_m	1.1	
f_{y_screw}	640	(8.8 screw)
A_{screw}	814	[mm^2]

Buckling capacity of U-profile:

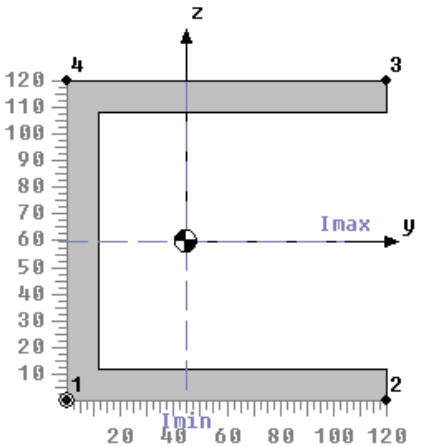

Cross-section of U-profile. Plate thickness 12 mm.

E	210	[GPa]	κ	**1.0**	($\lambda \leq 0.2$)
I_u (min.)	5869275	[mm^4]			
L_u	500	[mm]	γ_m	1.1	

$$N_{k\_u} = \frac{\pi^2 E I_u}{L_u^{\ 2}}$$

$$N_{Rd\_u} = \frac{\kappa f_{y\_u} A_u}{\gamma_m}$$

N_{k_u}	**48659**	[kN]	N_{Rd_u}	**1301**	[kN]
f_{y_u}	355	[MPa]			
A_u	4032	[mm$^{2]}$]			

$$\lambda = \sqrt{\frac{f_{y\_u} A_u}{N_{k\_u}}}$$

λ	**0.1715**

Fatigue calculation:

Z	1E+08	[m]	
Z_{sample}	160	[m]	
N_t	6.25E+05		Required
γ_{mf}	1.05		
ΔF	30 000	[N]	

$$N_t = \left(\frac{\Delta\sigma_c}{\gamma_{mf}\,\Delta\sigma_{Rd}}\right)^3 \cdot 2 \cdot 10^6$$

$\Delta\sigma_c$	36	[MPa]
A_u	4032	[mm^2]
$\Delta\sigma_{Rd}$	9.18	[MPa]
N_u	**1.04E+08**	cycles

Variants 3 & 4

Required bending resistance:

r_1	740	[mm]
r_3	550	[mm]
F_x	384	[kN]

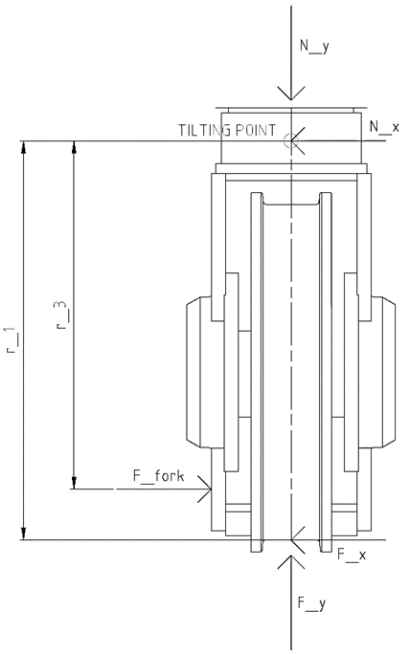

$\Sigma M=0$

$F_x r_1 - F_{fork} r_3 = 0$

$\Sigma F=0$

$F_x - F_{fork} + N_x = 0$ Horizontal

F_{fork}	**516.7**	[kN]

$$W = \frac{\gamma_m F_{fork} r_3}{\sigma_{y\_fork}}$$

γ_m	1.1	
σ_{y_fork}	355	[MPa]
W	**880496**	[mm^3]

Shear force capacity:

A_{fork}	**2778**	[mm^2]
γ_m	1.1	
F_{fork}	**516.7**	[kN]

$$\tau = \frac{\gamma_m F_{fork}}{A_{fork}}$$

τ	205	[MPa]
τ_{y_fork}	205	[MPa]

Fatigue calculation:

Z	1E+08	[m]	
Z_{sample}	160	[m]	
N_t	6.25E+05		Required
γ_{mf}	1.05		
ΔF_x	30 000	[N]	

$$N_t = \left(\frac{\Delta\sigma_c}{\gamma_{mf}\,\Delta\sigma_{Rd}}\right)^3 \cdot 2 \cdot 10^6$$

$$\Delta\sigma_{Rd} = \frac{\Delta F_{fork} r_3}{W}$$

$\Delta\sigma_c$	36	[MPa]
$\Delta\sigma_{Rd}$	25.21	[MPa]
N_{fork}	**5.03E+06**	cycles

Problem of upside down fork structure:

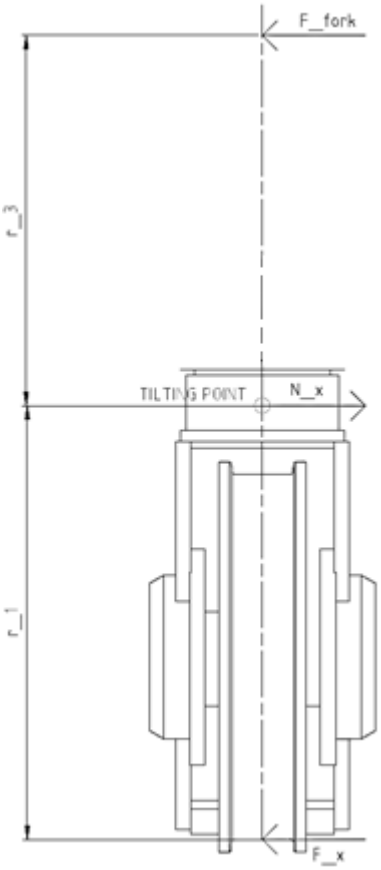

$\Sigma M=0$

$F_x r_1 - F_{fork} r_3 = 0$

$\Sigma F=0$

$F_x + F_{fork} - N_x = 0$ Horizontal

$\boldsymbol{N_x = F_x + F_{fork}}$

Cross-sections of fork structure.

Property 1 : Untitled
T Section
==========
AREA
A = 17875.
MOMENTS OF INERTIA
Izz = 105976302.
Iyy = 238786977.
Izy = 0.
PRINCIPAL INERTIAS
Max, I1 = 238786977.
Min, I2 = 105976302.
Polar, Ip = 344763279.
Angle, Alpha = 180.
RADIUS OF GYRATION
y = 115.5799
z = 76.99834
CENTROID FROM ORIGIN
H = 185.
V = 268.2343
STRESS RECOVERY LOCATIONS
1 H = 172.5
V = 0.
2 H = 197.5
V = 0.
3 H = 370.
V = 370.
4 H = 0.
V = 370.

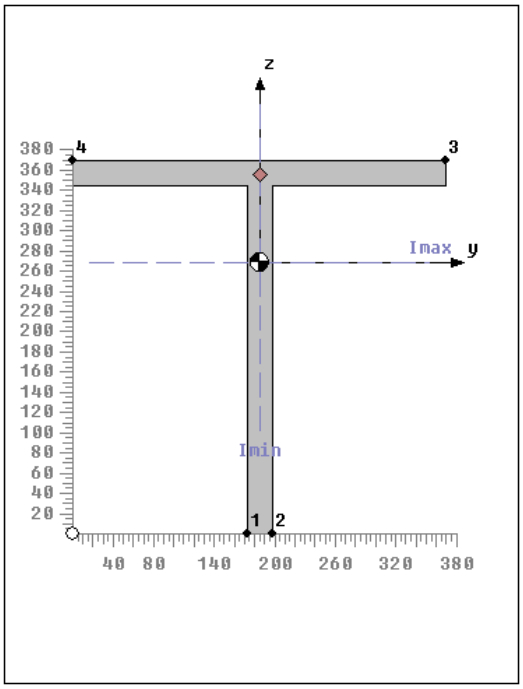

Property 1 : Untitled
I-Beam or Wide Flange (W)
==========
AREA
A = 16130.
MOMENTS OF INERTIA
Izz = 117715957.
Iyy = 123861659.
Izy = 2.98023E-8
PRINCIPAL INERTIAS
Max, I1 = 123861659.
Min, I2 = 117715957.
Polar, Ip = 241577616.
Angle, Alpha = 180.
RADIUS OF GYRATION
y = 87.62969
z = 85.42805
CENTROID FROM ORIGIN
H = 185.
V = 81.28797
STRESS RECOVERY LOCATIONS
1 H = 0.
V = 0.
2 H = 370.
V = 0.
3 H = 275.
V = 220.
4 H = 95.
V = 220.

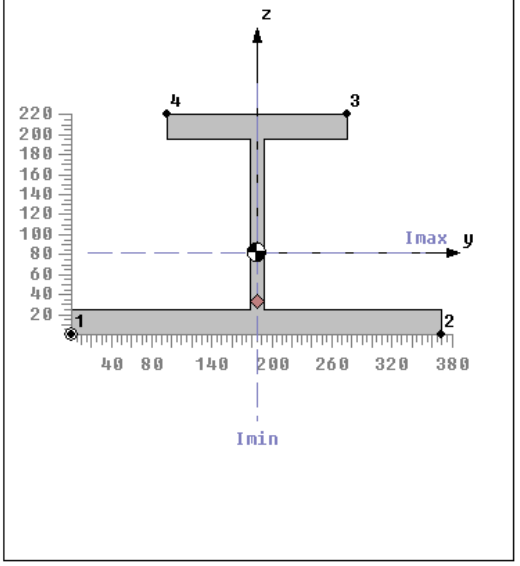

$$W = \frac{I_{fork}}{c}$$

	T	H	
I_{fork} (y-y)	2.39E+08	1.2E+08	[mm^4]
c	268.23	139	[mm]
W	890232	891091	[mm^3]

Appendix IV

Calculation of pot bearing fixing components.

Shear force capacity:

Screw	M16 8.8	
f_{y_screw}	640	[MPa]
A_{screw}	201	[mm^2]
γ_m	1.1	
γ_{sbs}	1.3	

$$F_{v,Rd} = \frac{f_{y\_screw} A_{screw}}{\gamma_m \gamma_{sbs} \sqrt{3}}$$

$F_{v,Rd}$	51.9	[kN]	(1 screw)
$F_{v,Rd}$	103.9	[kN]	(2 screws)

103 > 97.6 kN **OK**

Bearing capacity of screw and fixing plate connection:

σ_{y_fork}	355	[MPa]
d	16	[mm]
t	25	[mm]
γ_m	1.1	
γ_{sbb}	1.3	

$$F_{b,Rd} = \frac{\sigma_{y\_fork} dt}{\gamma_m \gamma_{sbb}}$$

$F_{b,Rd}$	99.3	[kN]

99.3 > 97.6 kN **OK**